

# Indirect searches for dark matter

M. Nicola Mazziotta

INFN-Bari

[mazziotta@ba.infn.it](mailto:mazziotta@ba.infn.it)

2013 Lepton Photon

# Dark Matter

See:

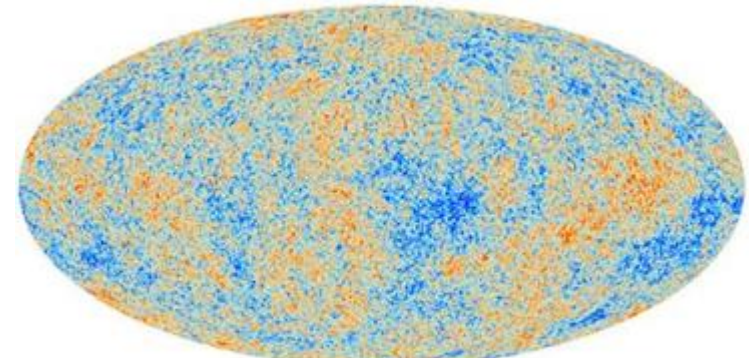
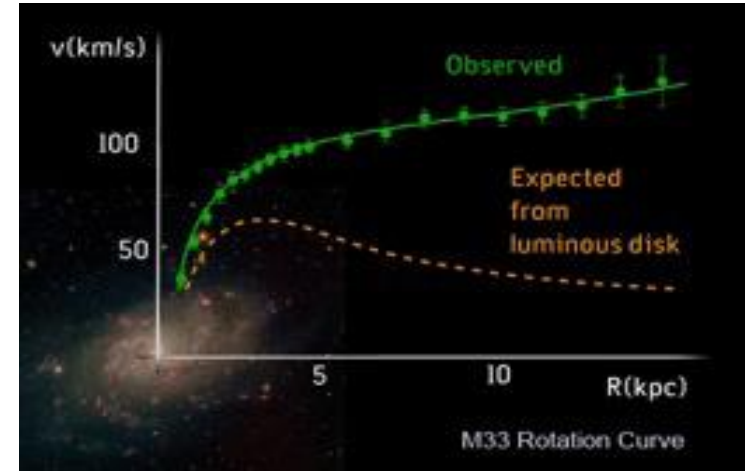
F. Bouchet talk

S. Das talk

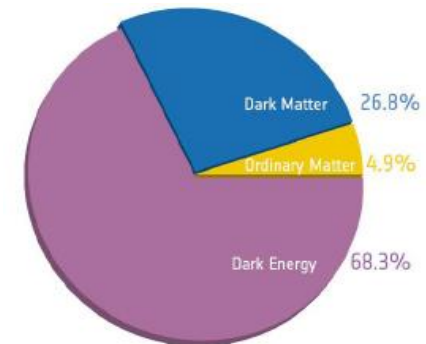
J. Frieman talk

S. Ritz talk

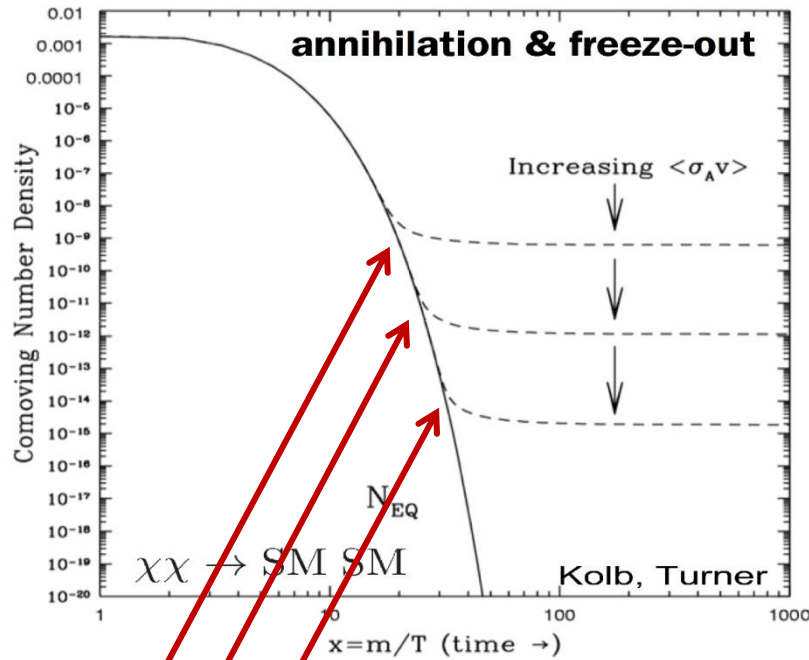
- Astrophysical evidence for missing mass
  - Galaxy rotation curves
  - Colliding clusters
  - Cosmological probes ( $\Omega_{dm} h^2 \approx 0.1$ )
- Observational evidence indicates:
  - Non-baryonic
  - (Almost totally) neutral
  - (Almost totally) collisionless
- Theoretical candidates:
  - Axions, sterile neutrinos, etc.
  - Modifications to gravity
  - Weakly Interacting Massive Particles (WIMPS)



Planck Collaboration, 2013



# WIMPs



Freeze-out:

$$\Gamma_{\text{ann}} = n \langle \sigma v \rangle \sim H$$

annihilation rate  $\sim$  expansion rate

$$\langle \sigma v \rangle_{\text{ann}} \sim 3 \times 10^{-26} \text{ cm}^3/\text{s for thermal relic}$$

- A WIMP in chemical equilibrium in the early universe naturally has the right density to be Cold Dark Matter
  - At early times, WIMPs are produced in  $l+l$ , ... collisions in the hot primordial soup (*thermal production*)
  - WIMP production ceases when the production rate becomes smaller than the Hubble expansion rate (*freeze-out*)
  - After freeze-out, the number of WIMPs per photon is constant
- Standard relic density calculation yields for nonrelativistic relics

$$\Omega_{\text{dm}} h^2 \approx \frac{3 \times 10^{-27} \text{ cm}^3 \text{ s}^{-1}}{\langle \sigma v \rangle} \simeq 0.1$$

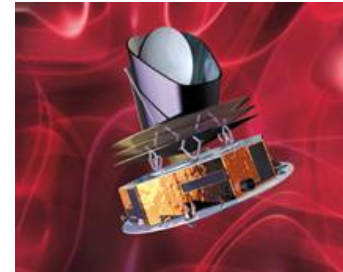
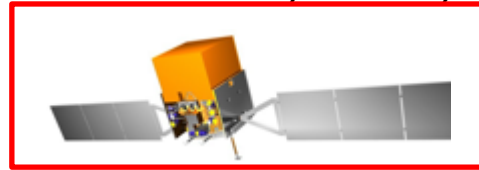
- Electroweak cross-sections are in correct range

$$\langle \sigma v \rangle \sim \frac{\alpha^2}{(200 \text{ GeV})^2} \sim 10^{-26} \text{ cm}^3 \text{ s}^{-1}$$

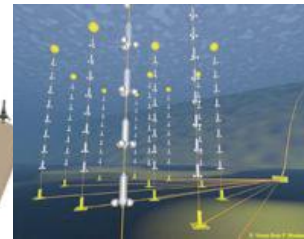
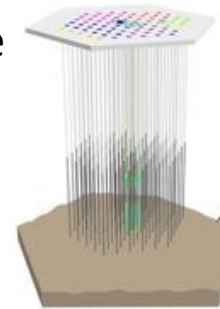
# Indirect Dark Matter Search



Ground based instrument:  
Cherenkov detector as HESS;  
MAGIC, VERITAS, ...  
Space satellite:  
Fermi-LAT, WMAP, PLANK, ...



IceCube  
Antares



- Annihilation or decay of dark matter can produce a variety of potentially detectable Standard Model particles
  - Contribute to cosmic rays
- Spectrum of annihilation (or decay) products encodes info about intrinsic particle properties
- Variation in the intensity of the signal along different lines of sight is determined exclusively by the distribution of dark matter

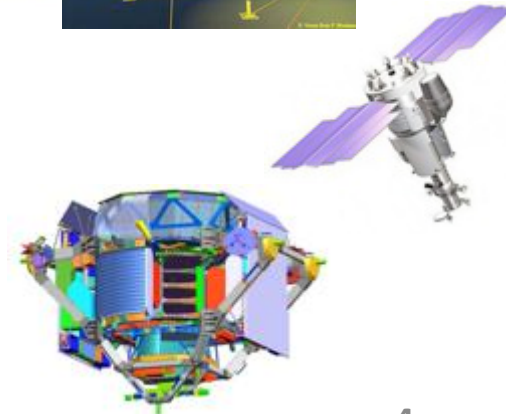
See D. Grant talk ...

B-field

See P. Zuccon talk

e+, anti-p, ...

PAMELA  
AMS-02  
Fermi-LAT



# Indirect WIMP Signatures: gamma-rays

Observed  
flux

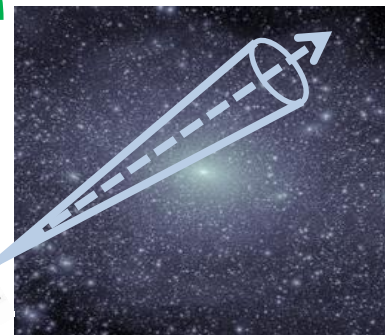
Intrinsic Particle  
Properties

Astrophysics

$$\text{ann. } \phi(E, \Delta\Omega) = \frac{1}{4\pi} \frac{\langle\sigma v\rangle}{2 m_\chi^2} \sum_f \frac{dN_f}{dE} B_f \int_{\Delta\Omega} d\Omega \int_{l.o.s.} dl \rho^2(l(\Omega))$$

decay  $\Gamma_D/m_\chi$

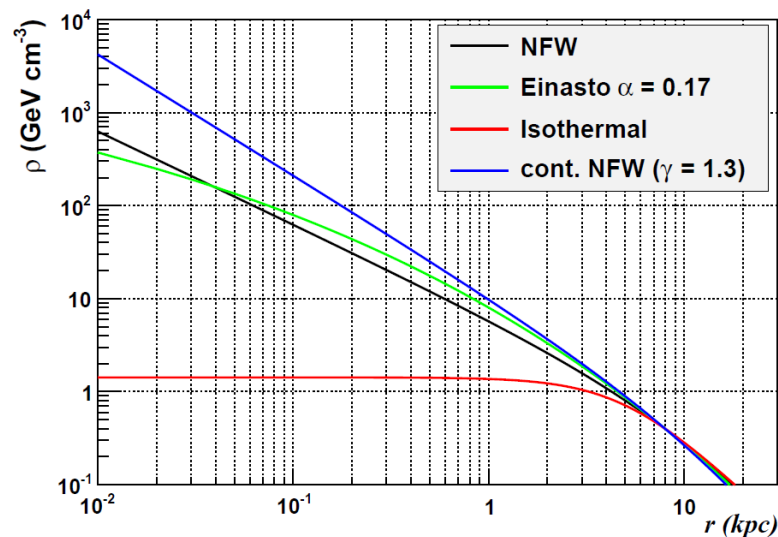
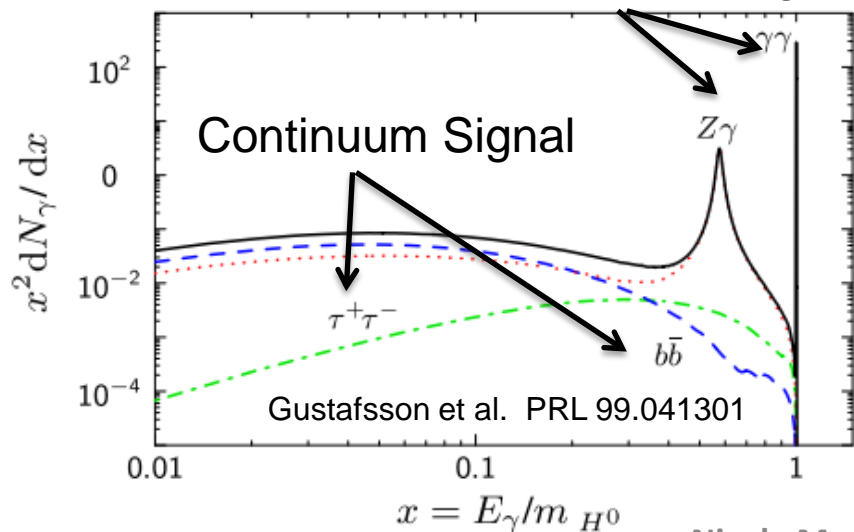
$\rho(l)$



$\langle\sigma v\rangle_{\text{ann}} \sim 3 \times 10^{-26} \text{ cm}^3/\text{s}$   
for thermal relic

J-factor – DM distribution  
(line-of-sight integral)

Monochromatic Signal



# The Fermi Large Area Telescope

## Public Data Release:

All  $\gamma$ -ray data made public within 24 hours (usually less)

## Si-Strip Tracker:

convert  $\gamma \rightarrow e^+e^-$   
reconstruct  $\gamma$  direction  
EM v. hadron separation

## Hodoscopic CsI Calorimeter:

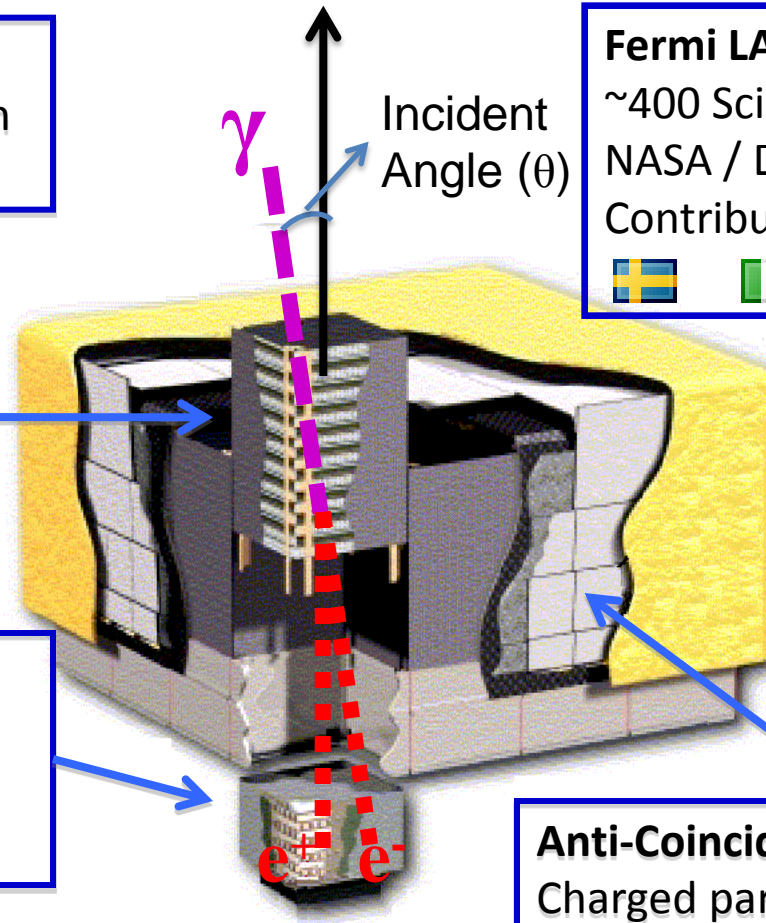
measure  $\gamma$  energy  
image EM shower  
EM v. hadron separation

## Trigger and Filter:

Reduce data rate from  $\sim 10\text{kHz}$  to 300-500 Hz

## Fermi LAT Collaboration:

$\sim 400$  Scientific Members,  
NASA / DOE & International  
Contributions



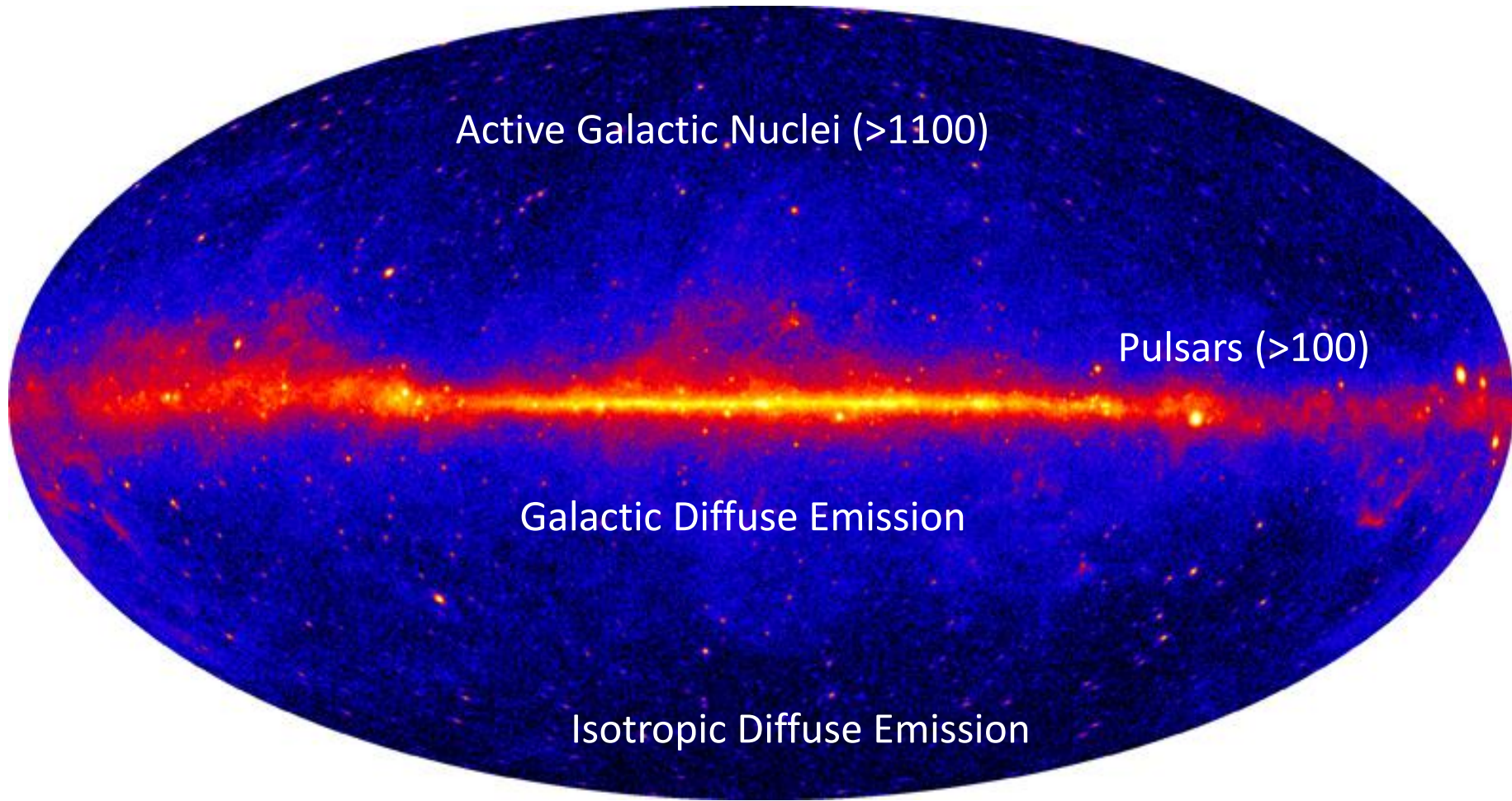
On orbit since  
June 11, 2008

**Anti-Coincidence Detector:**  
Charged particle separation

Atwood et al., ApJ 697, 1071 (2009)  
Ackermann et al. ApJS 203, 4 (2012)

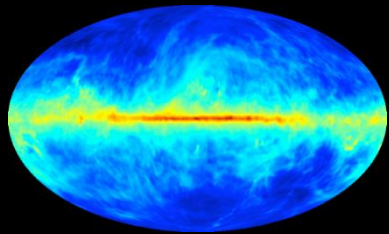
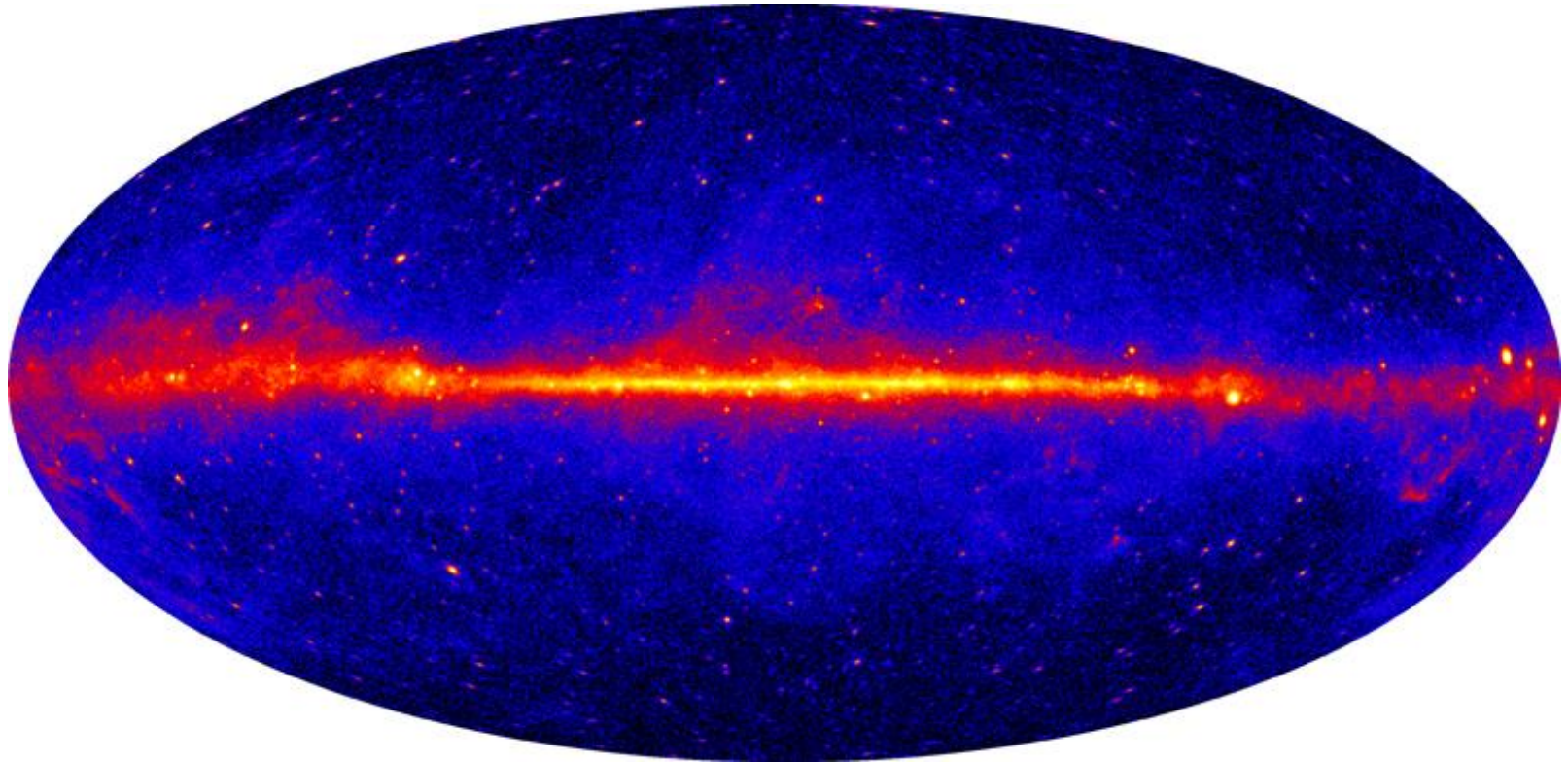
# Fermi-LAT Gamma-Ray Sky Map

Credit: NASA/DOE/International LAT Team

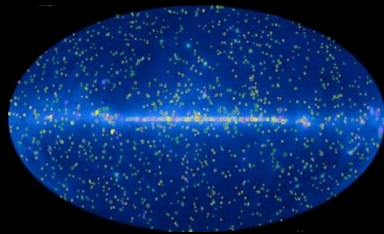


+Pulsar Wind Nebulae + Supernova Remnants + Globular Clusters + Starburst Galaxies + Unassociated Sources+ ...

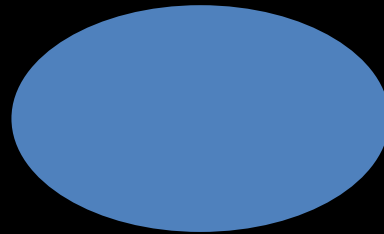
# Are there any hiding DM signals?



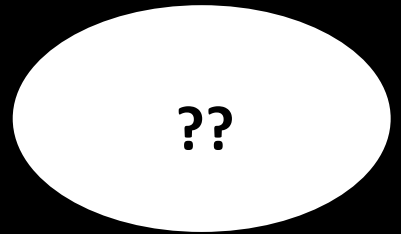
+



+



+



Galactic

Point Sources

Isotropic

.. DM signal



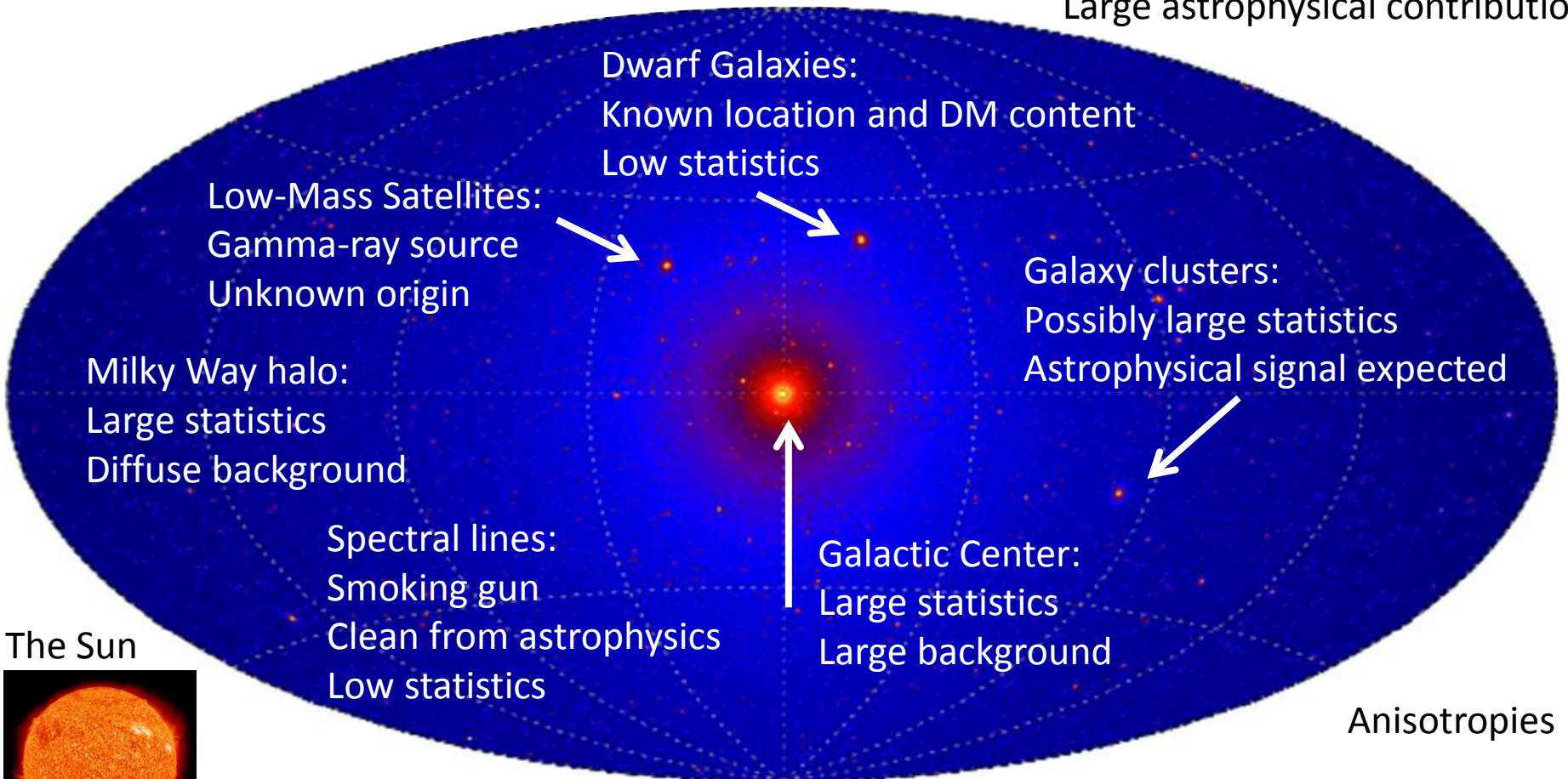
# Dark Matter Distribution: search targets

$$\int_{\Delta\Omega} d\Omega \int_{l.o.s.} dl \rho^2(l(\Omega))$$

Electrons/Positrons

Boost factor =  $\langle \rho^2 \rangle / \langle \rho \rangle^2$  depends on position and on statistics (shape, mass) of subhalos

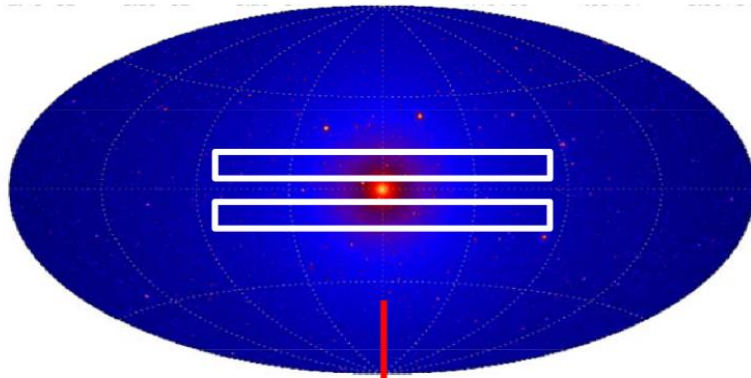
Extragalactic background:  
Large statistics  
Large astrophysical contribution



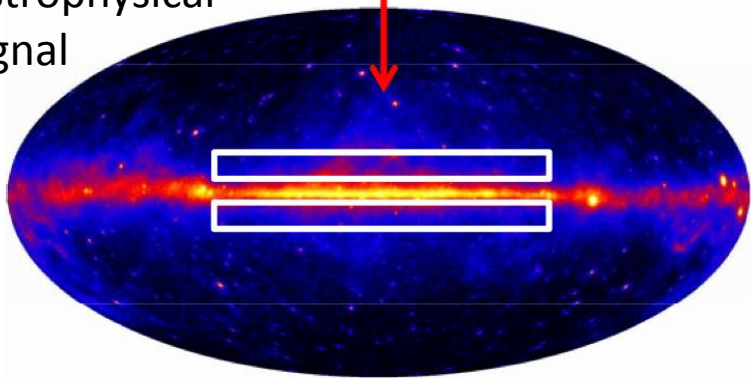
# Milky Way Dark Matter Halo

Search for emission from annihilating or decaying DM from the inner extended Milky Way DM halo [Ackermann+ ApJ 761 (2012) 91]

Expected DM signal

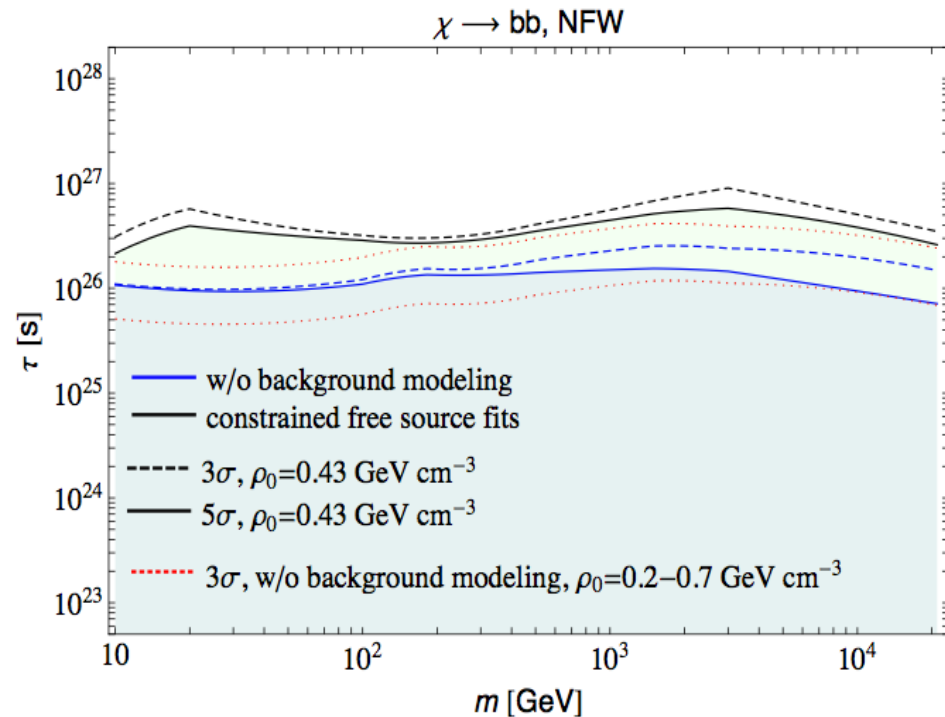
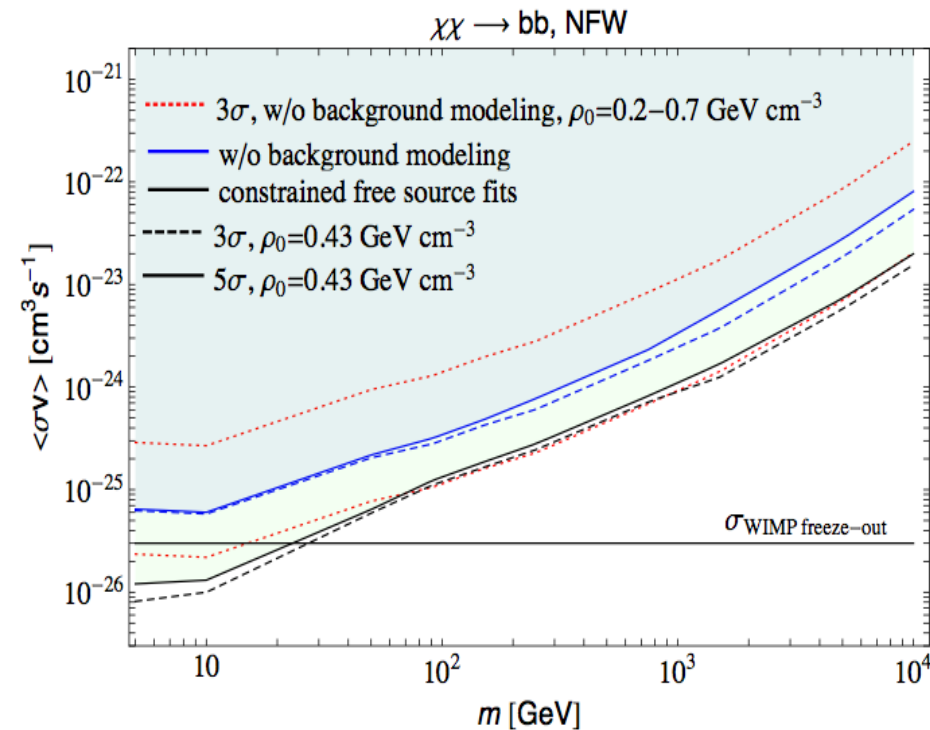


Astrophysical signal



- Analyze two 10 degree bands 5 degrees off the plane
  - to decrease astrophysical background
  - to mitigate uncertainties from inner DM density profile
- Two approaches to set limits:
  1. more conservative: assume emission only from DM
  2. more accurate: fit the DM and astrophysical emission simultaneously

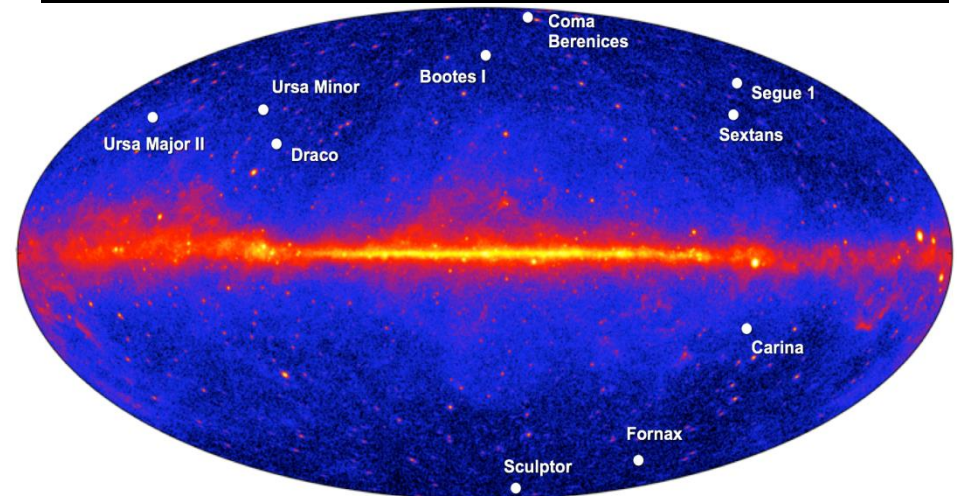
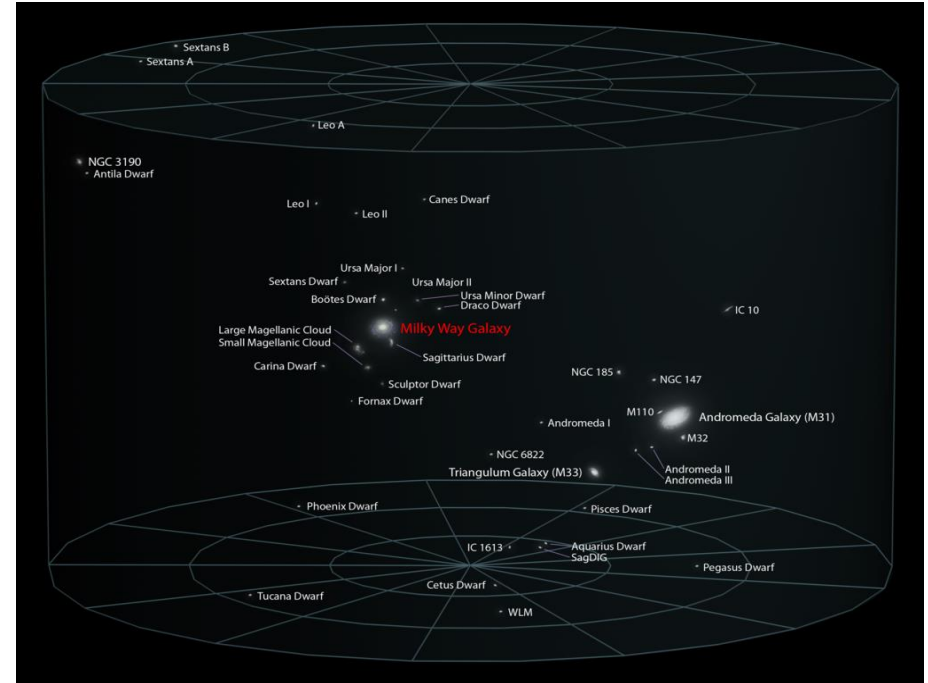
# Constraints from Milky Way Halo



- Including modeling of the astrophysical emission improves the DM constraints by a factor of  $\sim 5$
- With inclusion of astrophysical backgrounds, the limit constrains a canonical thermal annihilation cross section into b-quarks to a WIMP mass  $\gtrsim 30 \text{ GeV}$

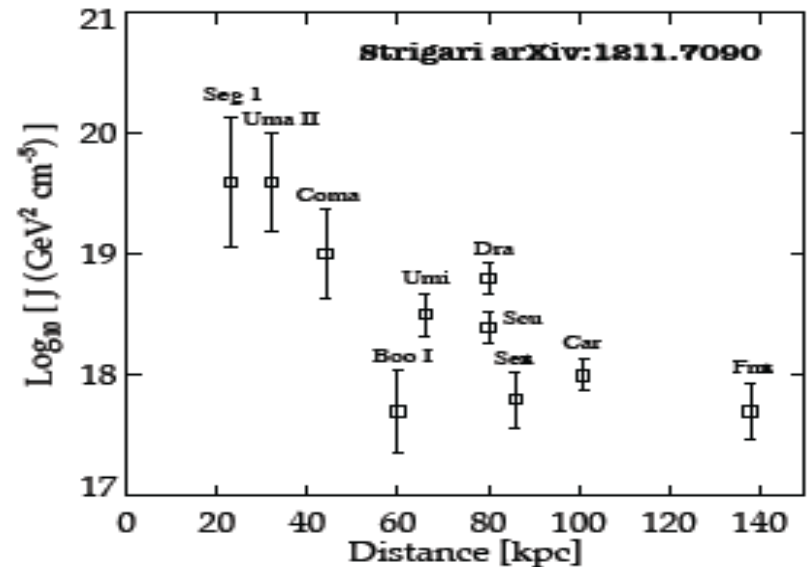
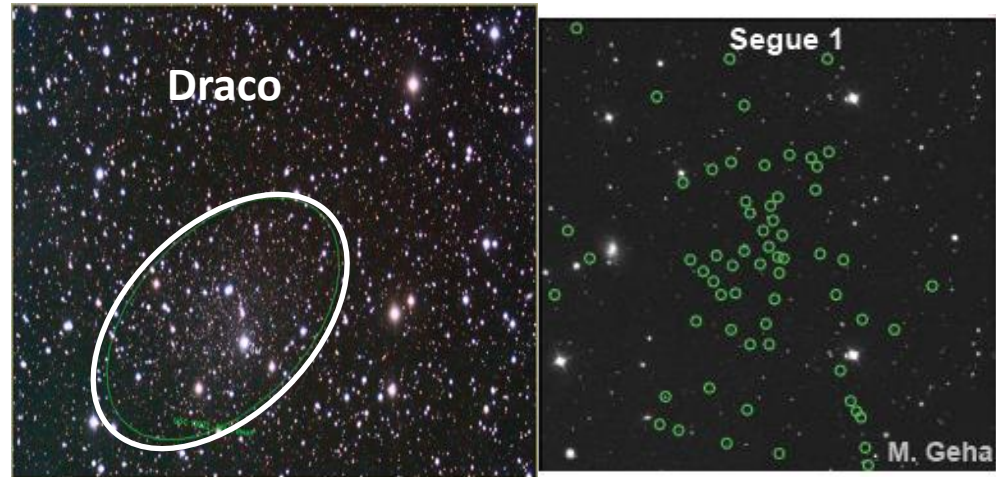
# Dwarf Spheroidal Galaxies

- Most dark-matter dominated objects in the universe (100 - 1000 times more dark matter than visible matter)
- Relatively close (25 - 150 kpc)
- High Galactic latitudes (minimize astrophysical foregrounds)
- Multi-wavelength observations show no mechanism for astrophysical gamma-ray production
  - No active star formation (no energy injection)
  - No appreciable magnetic fields (no acceleration)
  - No gas or dust (no target material)



# dSph Dark Matter Content

- Dark matter content determined from stellar velocity dispersion
  - Classical dwarfs: spectra for several thousand stars
  - Ultra-faint dwarfs: spectra for fewer than 100 stars
- Fit dark matter profile from the stellar velocity distribution of each dwarf
- Estimate the dark matter content and uncertainty
- Combine observations of multiple dwarf galaxies to improve search sensitivity, including the DM uncertainty



# Dwarf Spheroidal Summary

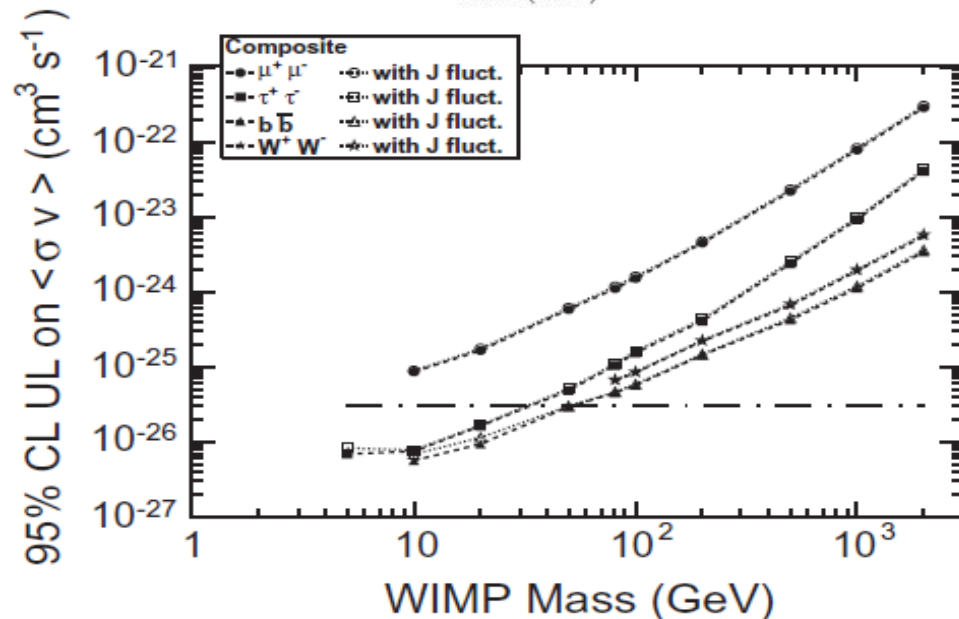
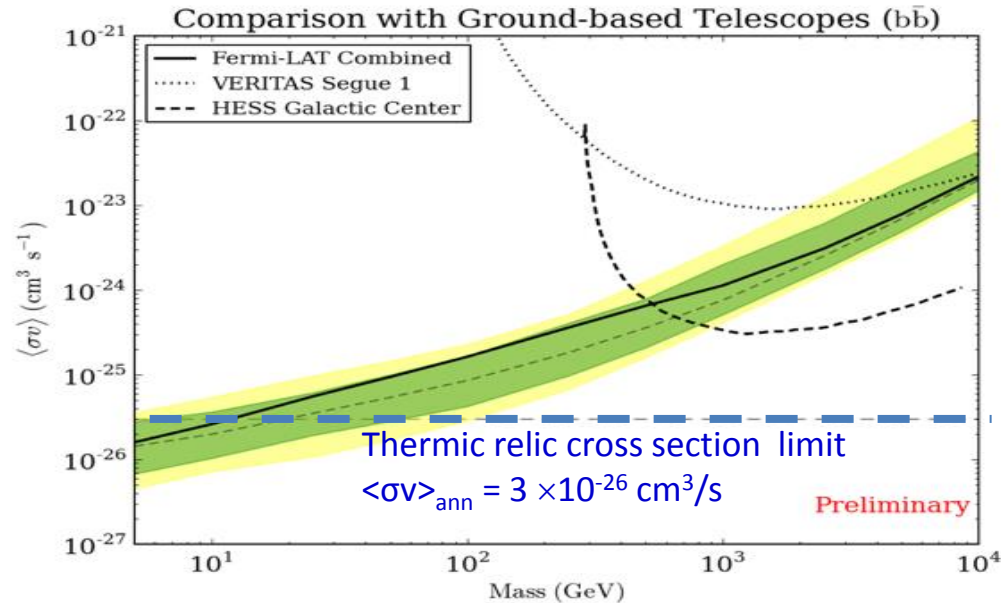
- 3-4 years of Fermi-LAT data from 10 dwarf spheroidal galaxies constrain the thermal relic cross section for low mass dark matter
- Comparable to limits from ACT observations of dwarf galaxies for high-mass dark matter.
- Currently, statistically limited (especially at high masses).
- Many dwarf galaxies remain to be discovered in optical surveys of the southern hemisphere.

Ackermann et al., arXiv:1108.3546

Geringer-Sameth et al., arXiv:1108.2914

MNM et al., arXiv:1203.6731

...



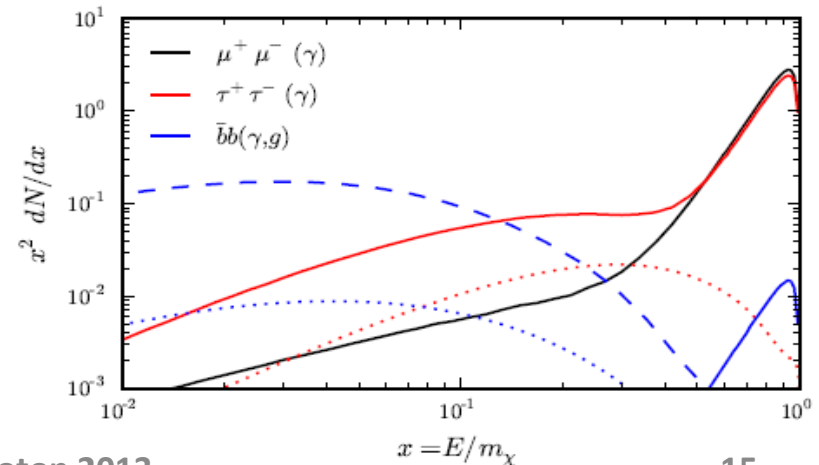
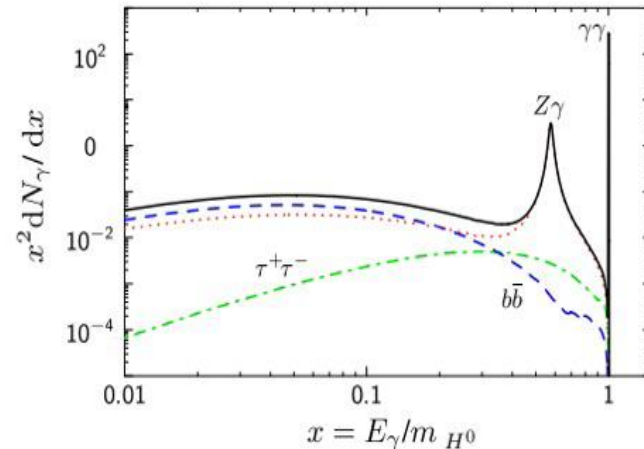
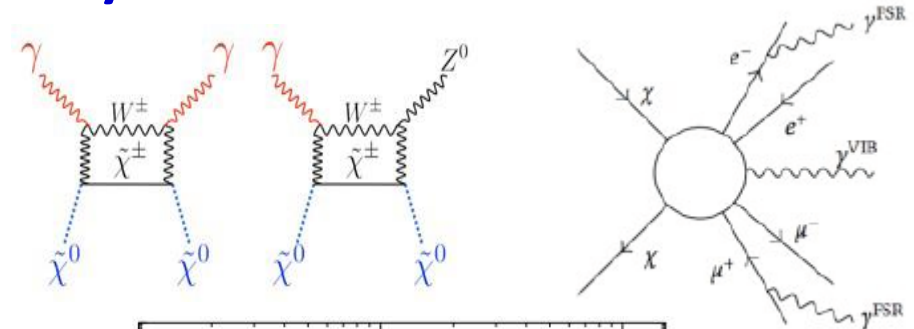
# Gamma-ray lines

- Annihilation into  $\gamma\gamma$  or  $\gamma X$  ( $X = Z^0, H^0, \dots$ ) at loop level  $O(\alpha^2)$  or Virtual internal bremsstrahlung (VIB) at loop level  $O(\alpha)$  will produce a distinct spectral feature

- Clean signal (hard to mimic with astrophysics)  $\rightarrow$  Smoking gun signal!
- Low statistics (suppressed by a factor of  $10^2$  to  $10^3$  in many models),  $\langle\sigma v\rangle_{\gamma\gamma} \sim 10^{-30} \text{ cm}^3/\text{s}$
- Different target regions according to the different DM profile

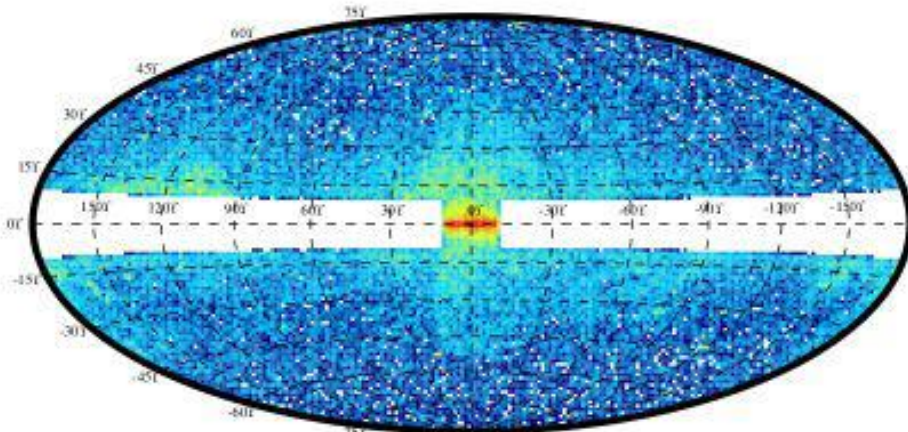
Bergstrom et al. Nucl. Phys. B504, 27 (1997)  
 Ferrer et al., Phys. Rev D74, 115007 (2006)  
 Gustafsson et al. PRL 99, 041301 (2007)  
 Profumo, Phys. Rev. D78, 023507 (2008)  
 Bringmann et al., arxiv::1203.1312 (2012)

...



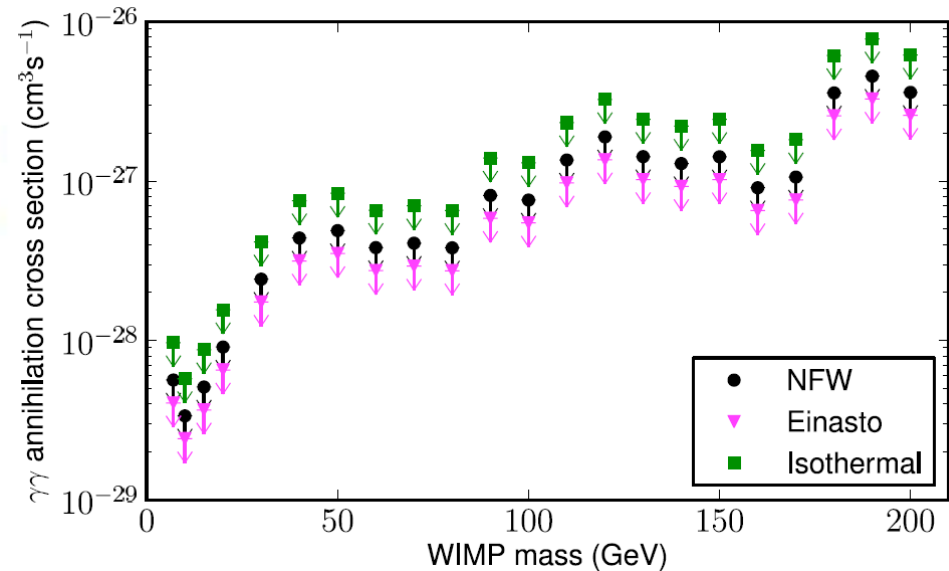
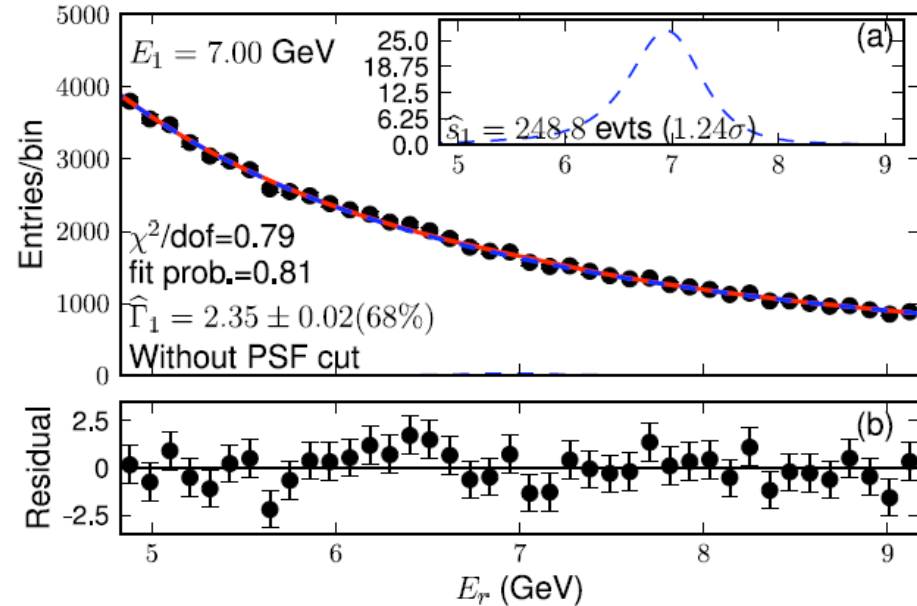
# Spectral line search

- Sliding window technique: model bkg as single power law and model energy dispersion from simulation ('line like' excess).
- 2 yr analysis Fermi LAT looked at the whole sky data and found no evidence of a line



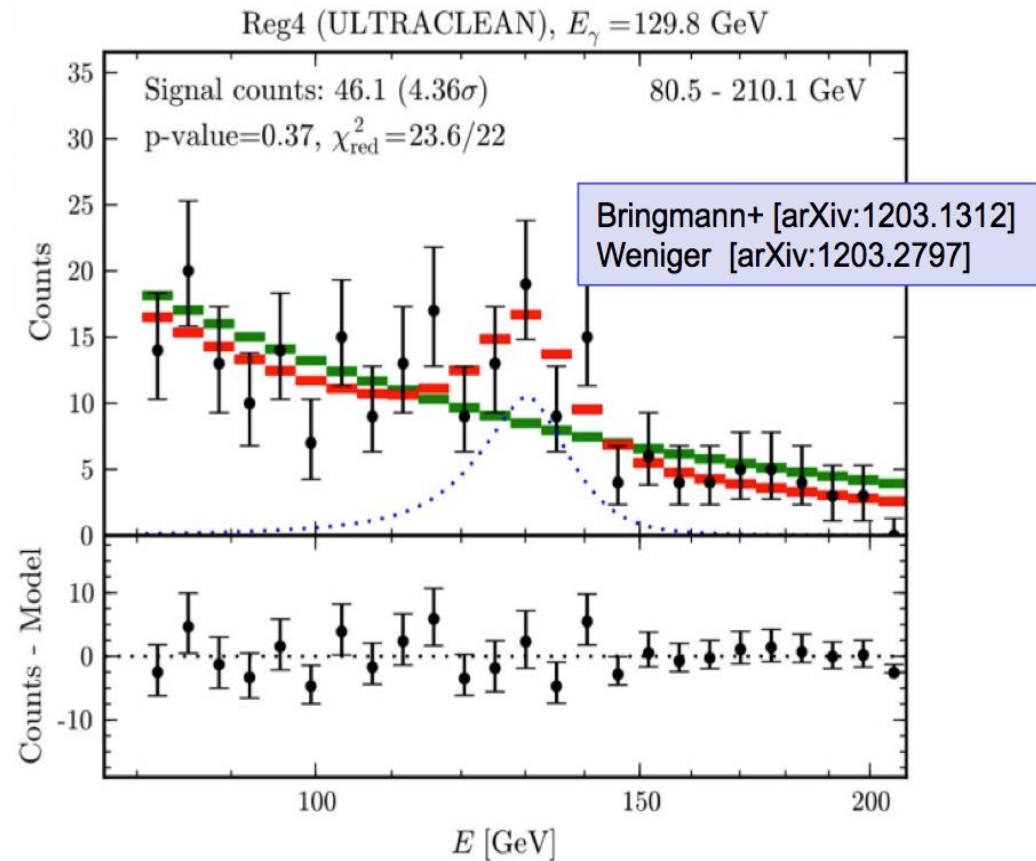
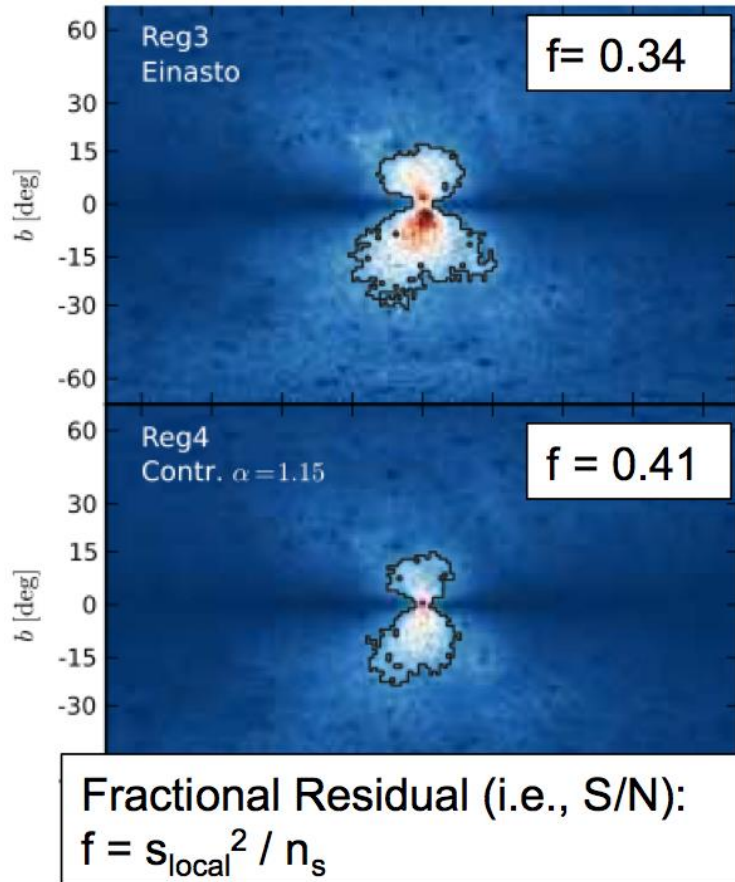
$|b| > 10^\circ$  plus  $|\ell|, |b| < 10^\circ$

M. Ackermann et al. (FERMI-LAT)  
PRD 86, 022002 (2012)  
arXiv:1205.2739





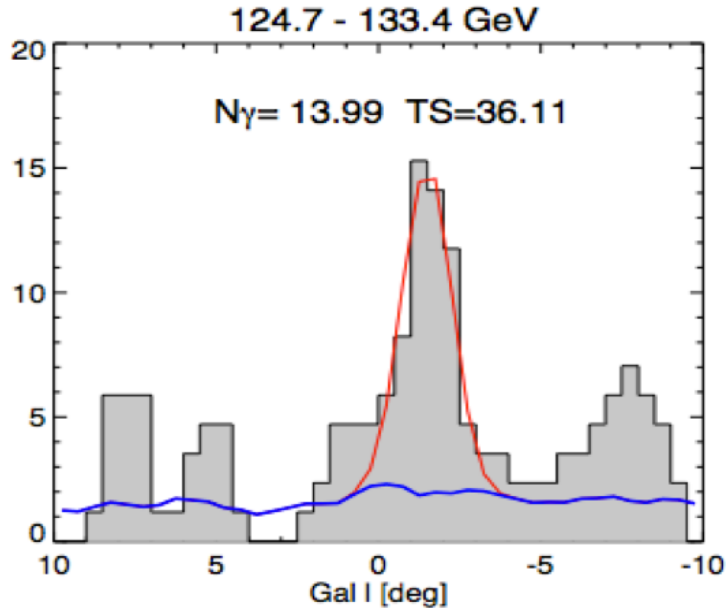
# Evidence for 130 GeV gamma-ray line?



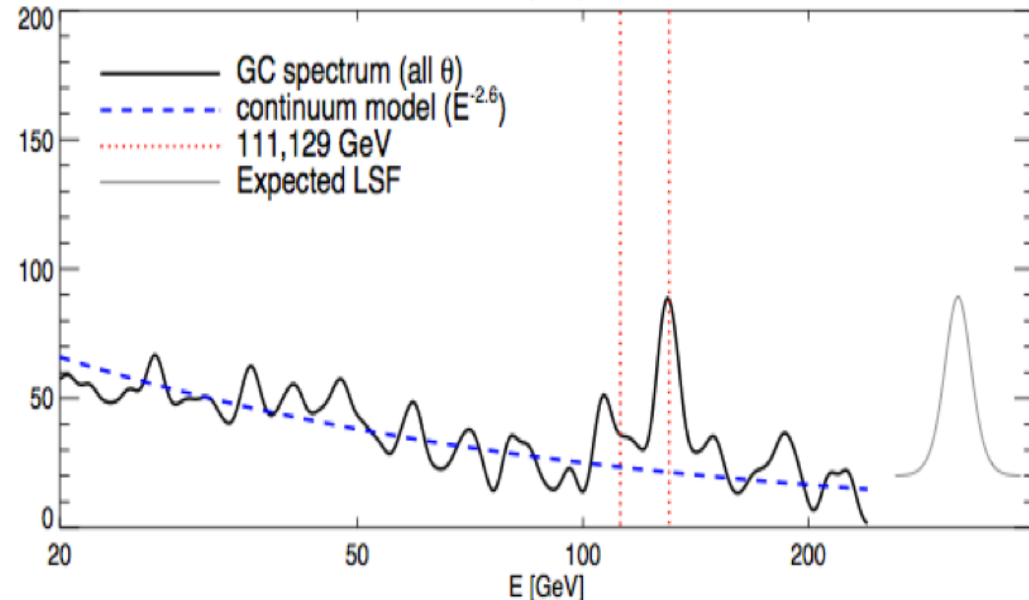
- Bringmann et al. and Weniger showed evidence for a narrow spectral feature near 130 GeV and near the Galactic centre:
  - Signal is particularly strong in 2 out of their 5 test sky regions, shown above.
  - $4\text{-}5\sigma$ (local), with S/N  $\approx 30\text{-}60\%$  in optimized regions of interest (ROI).

# Evidence for 130 GeV gamma-ray line?

## Gal. Long. Profile at ~130GeV



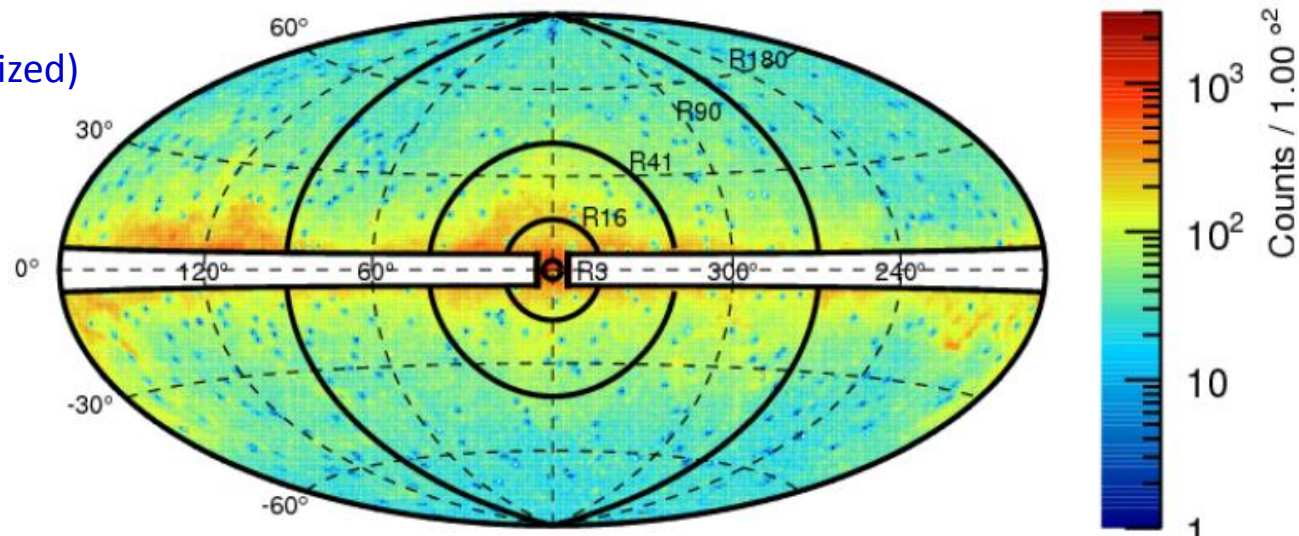
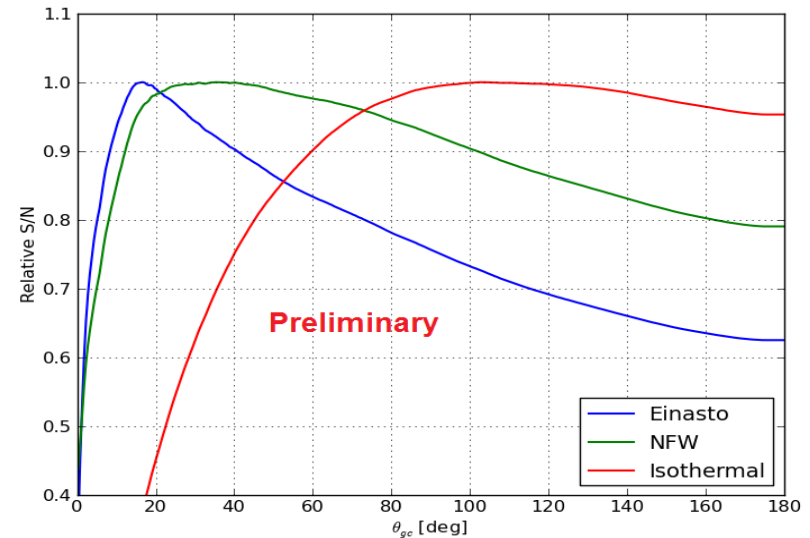
## Energy Spectrum from GC



- Su & Finkbeiner showed that the spectral feature was close to, but slightly ( $\sim 1.5$  deg) offset from, the Galactic centre [arXiv:1206.1616].
- Their likelihood analysis included a spatial morphology of signal, and data-driven model of Galactic astrophysical backgrounds.
- Claimed  $6\sigma$  statistical significance, after a trials factor of  $\sim 6000$ , but acknowledge uncertainties of modeling the Galactic astrophysical backgrounds.

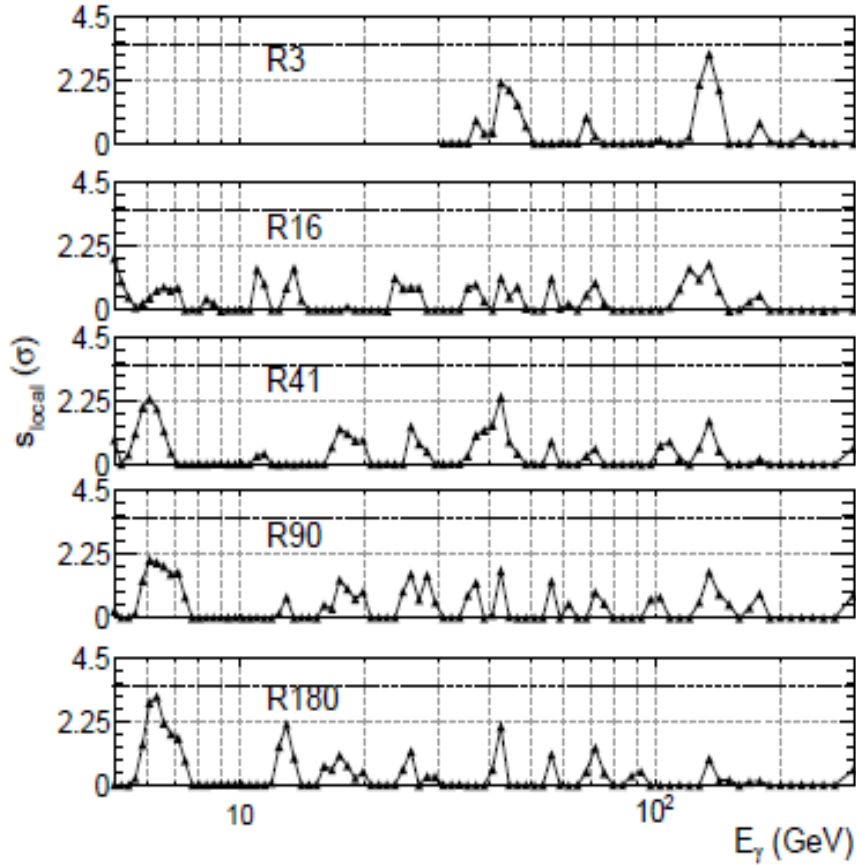
# Fermi-LAT Line Search - 4 years data

- Search for lines from 5 – 300 GeV using 3.7 years of data
- Use P7REP\_CLEAN (REP = “reprocessed”)
  - Mask bright ( $>10\sigma$  for  $E > 1$  GeV) 2FGL sources
- Optimize ROI for a variety of DM profiles
  - Find  $R_{GC}$  that optimizes  $S/\sqrt{B}$
- Search in 5 ROIs
  - R3 ( $3^\circ$  GC Circle, cont. NFW Optimized)
  - R16 (Einasto Optimized)
  - R41 (NFW Optimized),
  - R90 (Isothermal Optimized)
  - R180 (DM Decay)



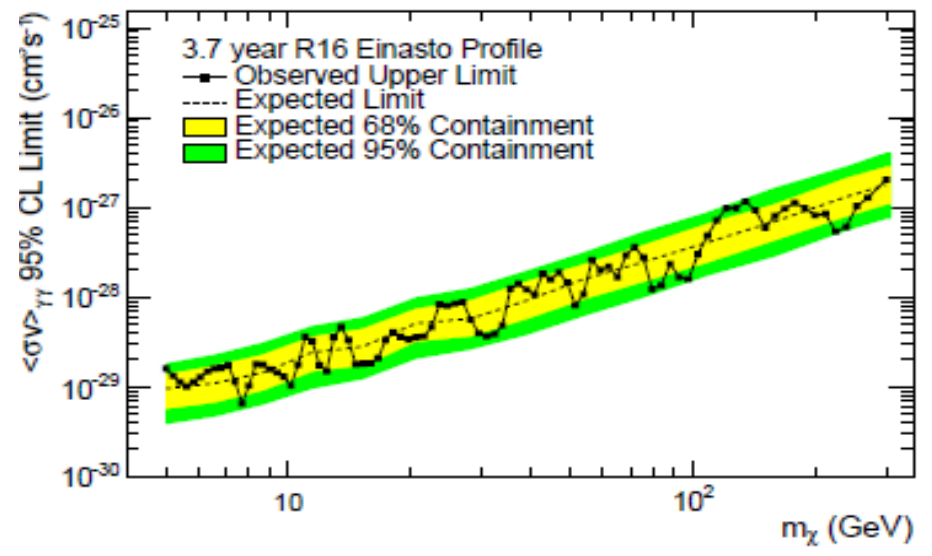
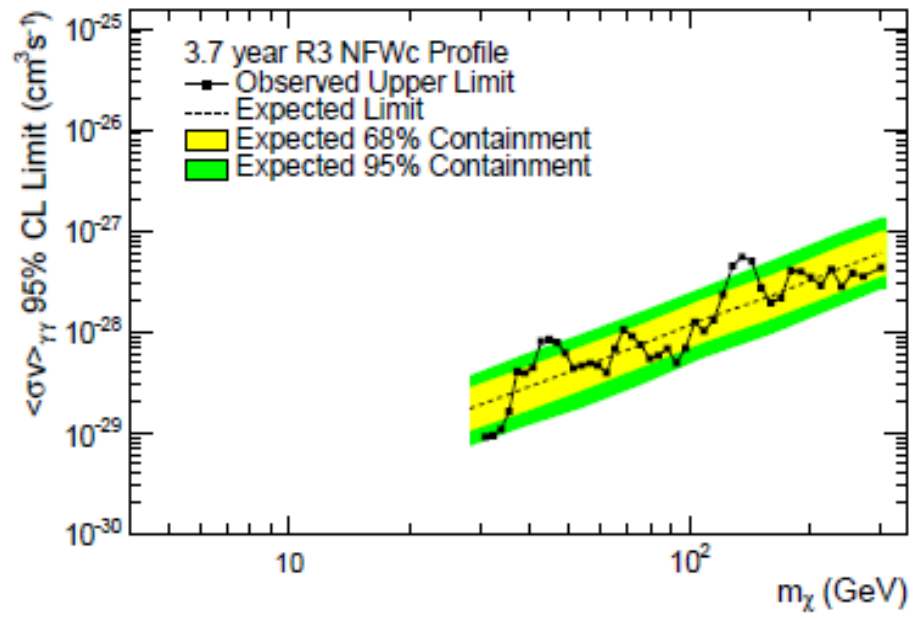
arXiv:1305.5597

# 95% CL $\langle\sigma v\rangle_{\gamma}$ Upper Limit R3-R16

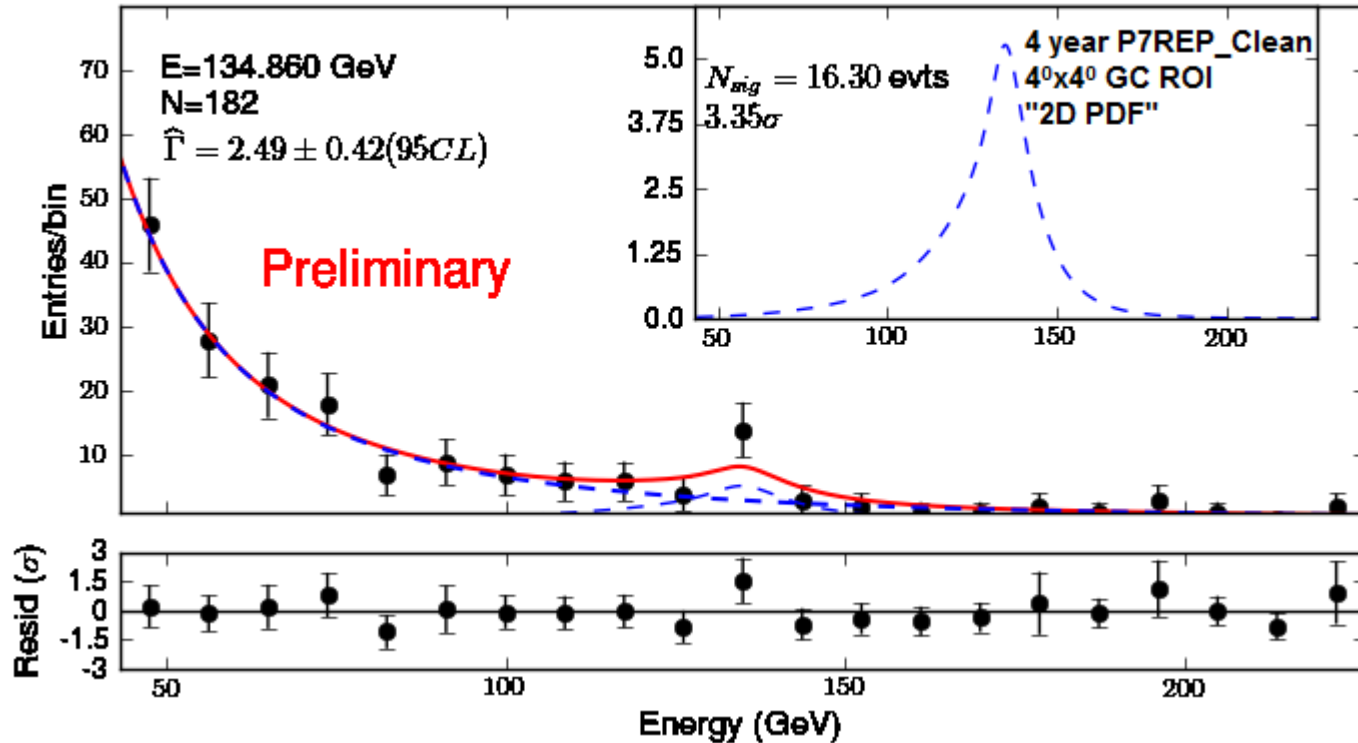


- No globally significant lines detected
  - All fits have global significance  $< 2\sigma$

arXiv:1305.5597

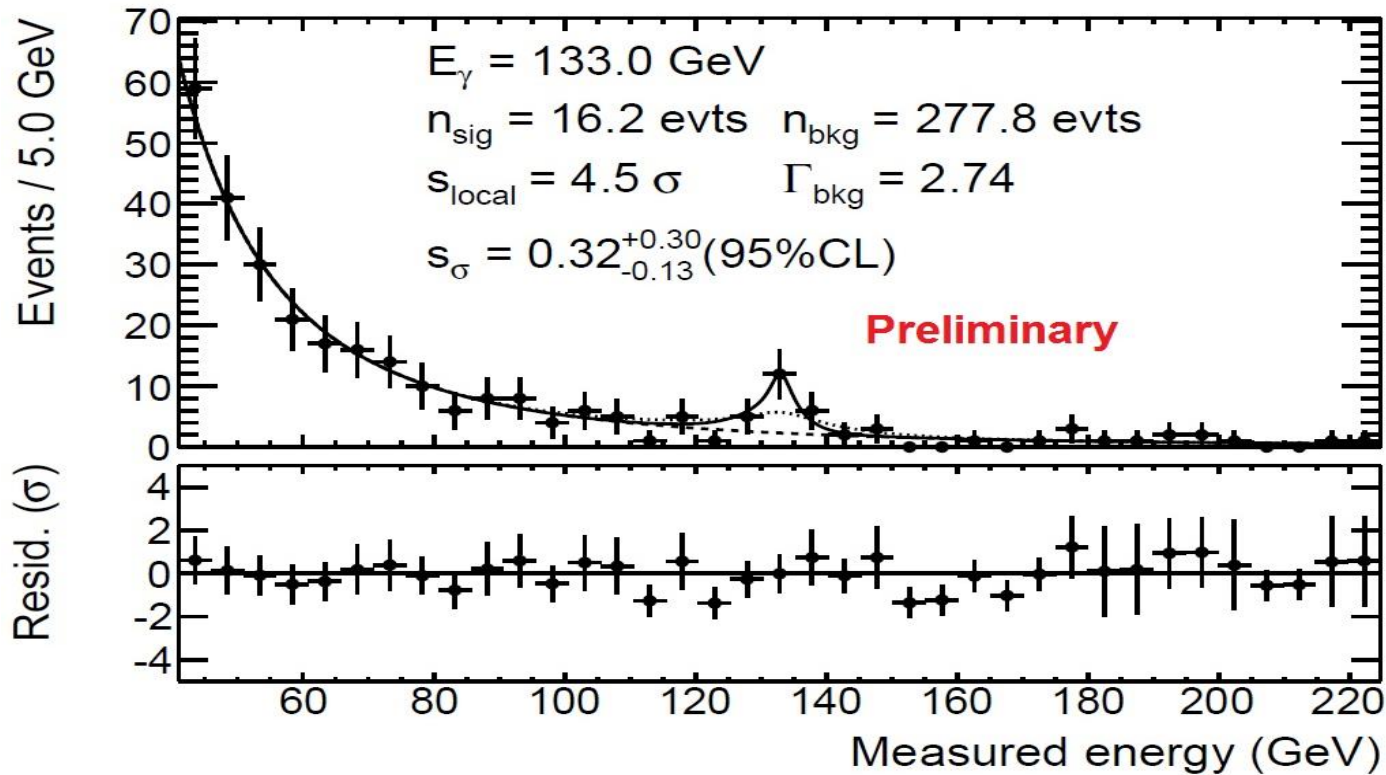


# Fermi-LAT Team Line Search at 135 GeV



- 4.01 $\sigma$  (local) 1D fit at 130 GeV with 3.7 year unprocessed data
  - Look in 4 $^{\circ}$ x4 $^{\circ}$ GC ROI, Use 1D PDF (no use of  $P_E$ )
- 3.73 $\sigma$  (local) 1D fit at 135 GeV with 3.7 year reprocessed data
  - Look in 4 $^{\circ}$ x4 $^{\circ}$ GC ROI, Use 1D PDF (no use of  $P_E$ )
- **3.35 $\sigma$  (local) 2D fit at 135 GeV with 3.7 year reprocessed data**
  - **Look in 4 $^{\circ}$ x4 $^{\circ}$ GC ROI, Use 2D PDF ( $P_E$  in data)**
  - **<2 $\sigma$  global significance after trials factor**

# Width of Feature near 135 GeV



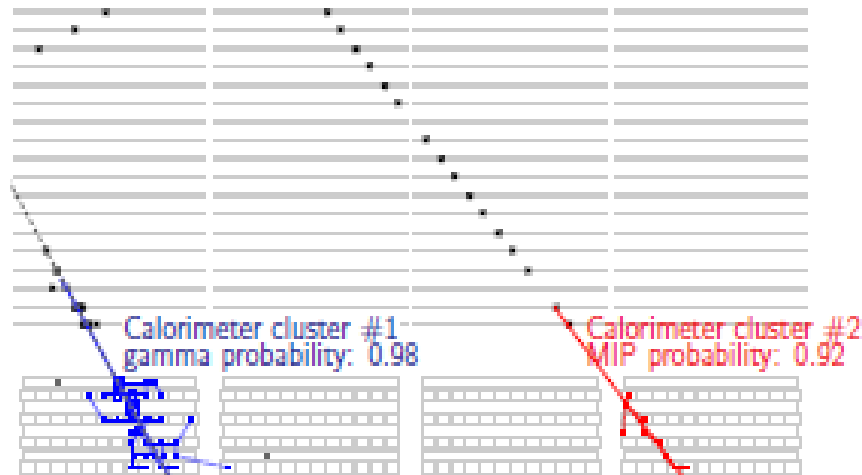
- Let width scale factor float in fit (while preserving shape)

$$s_\sigma = 0.32^{+0.30}_{-0.13} \text{ (95\% CL)}$$

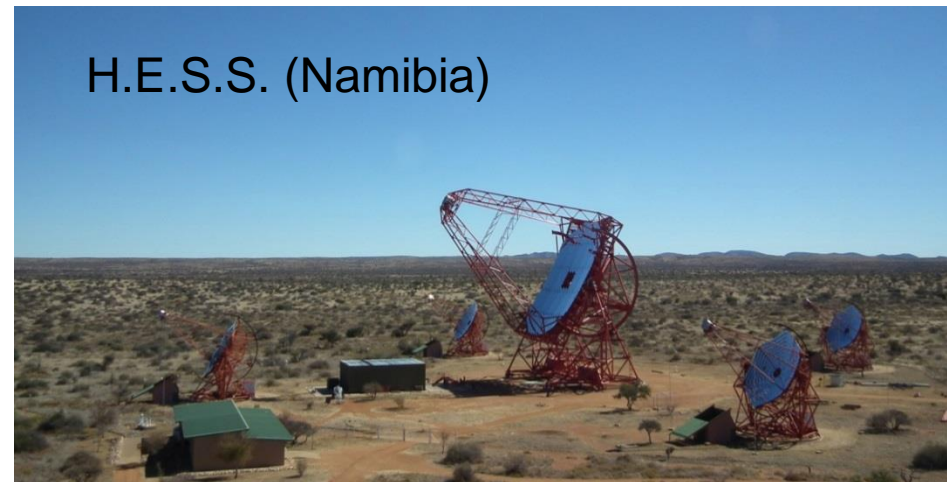
- Feature in data is narrower than expected energy resolution measured in beam tests and detector simulations

# Spectral line search: near terms prospect

- Fermi LAT: improved event analysis (Pass8) and weekly limb observations
  - Call for white papers on possible modifications to the observing strategy
- H.E.S.S. Cerenkov telescope: 50 hours of GC observation could be enough to rule out signature or confirm it at 5 sigma



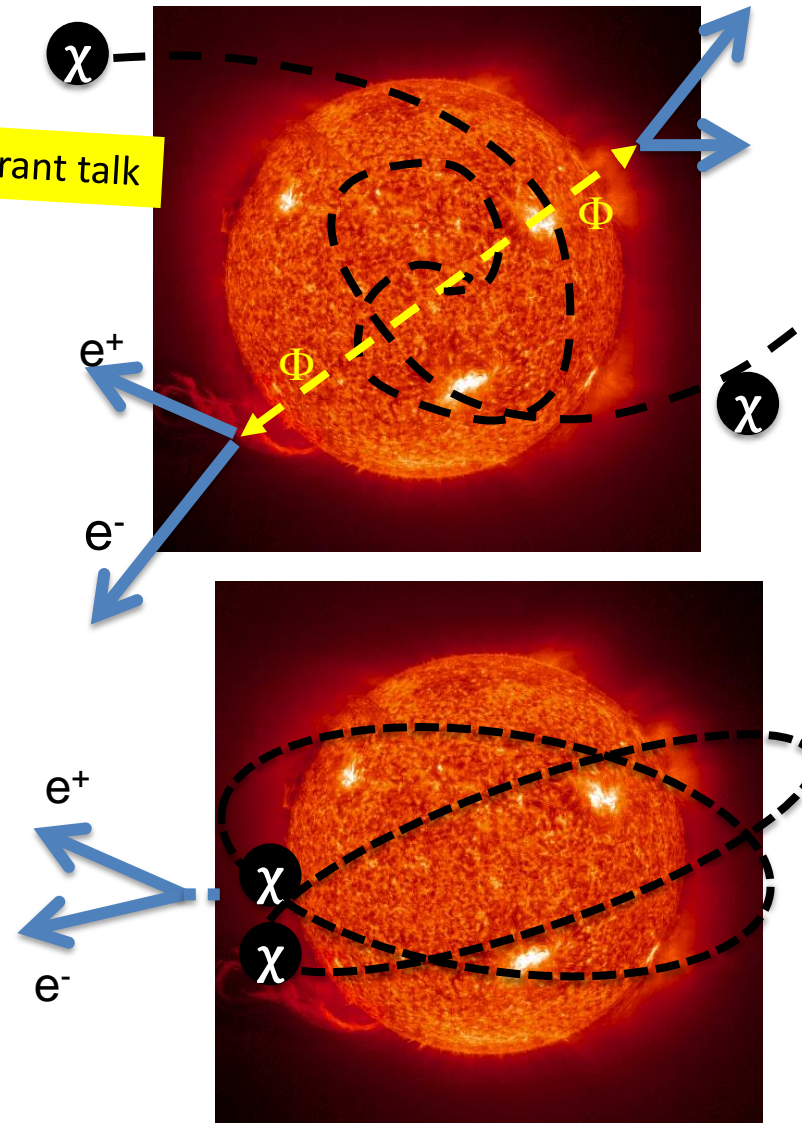
Fermi-LAT Upcoming Developments Pass 8



# Solar CREs from DM annihilation

- Combination of direct and indirect detection mechanisms
  - WIMP-nucleon scattering leads to WIMP capture by the Sun
  - WIMP-WIMP annihilation leads to the production of cosmic rays (e.g. neutrino )
- Charged particles (e.g. electrons and positrons) from DM capture and annihilation in the Sun core would not escape, but ...
- DM capture and annihilation through an intermediate state
  - WIMP accretion rate determined by scattering cross section
  - Annihilation through an intermediate particle  $\Phi$  that can travel out of the Sun and decay into cosmic rays
- DM captured through inelastic scattering and forms a loosely bound halo around the Sun
  - WIMP accretion via inelastic scattering (maintain large orbits)
  - Annihilation directly into cosmic-ray electrons in the solar neighborhood
- See P. Schuster et al., PRD 82, 115012 (2010)

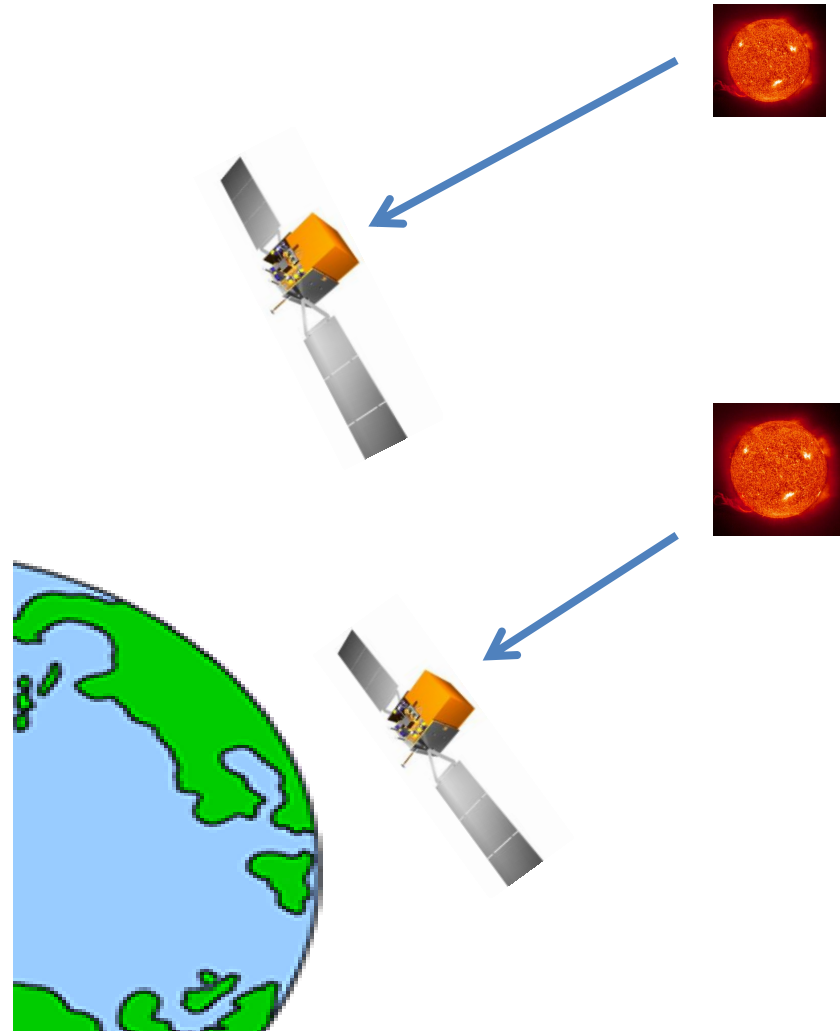
See D. Grant talk





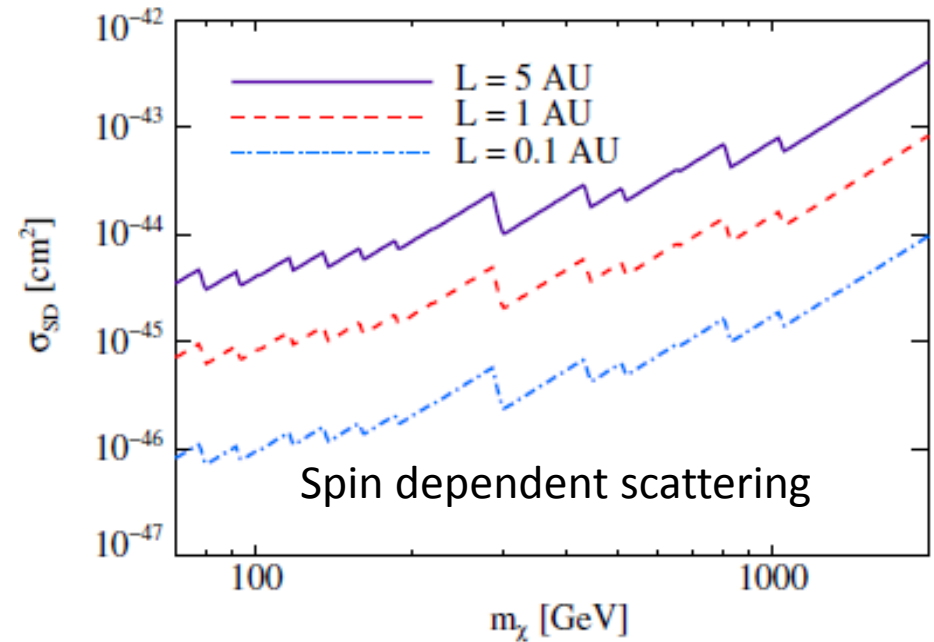
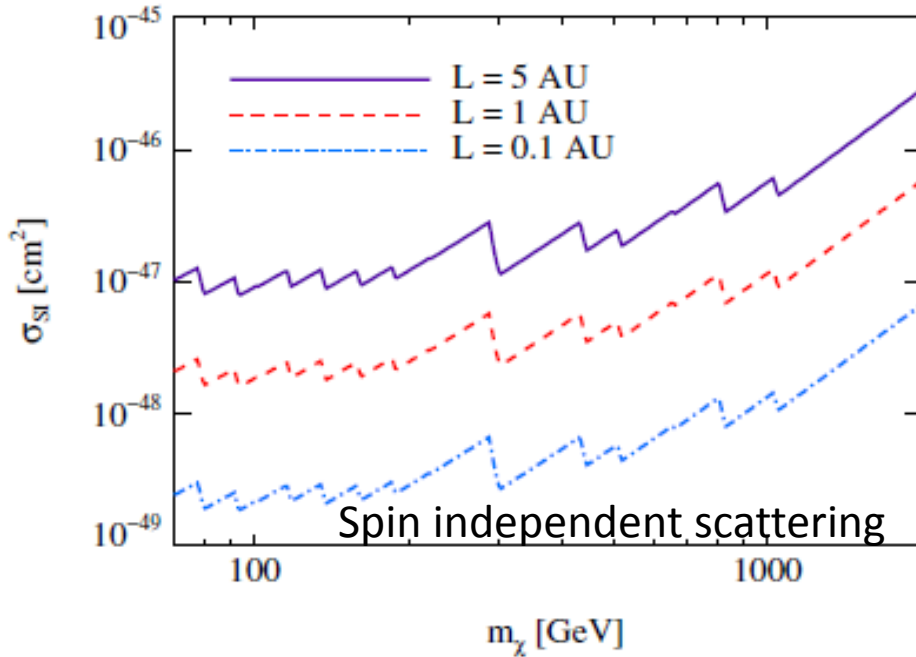
# CRE from the Sun: Fermi LAT results

- $\sim 10^6$  CRE events ( $E > 60$  GeV), from 1st year of operation
- Analysis performed in ecliptic coordinates, in reference frame centered on the Sun
  - Fake template centered in opposite direction or shuffling the arrival directions
  - Extended sky regions centered on the Sun with angular radii of  $30^\circ$ ,  $45^\circ$ ,  $60^\circ$  and  $90^\circ$  have been considered because the CRE trajectories could be affected by the geomagnetic and heliospheric magnetic field
- Search for a flux excess correlated with Sun's direction yielded no significant detection, flux upper limits placed



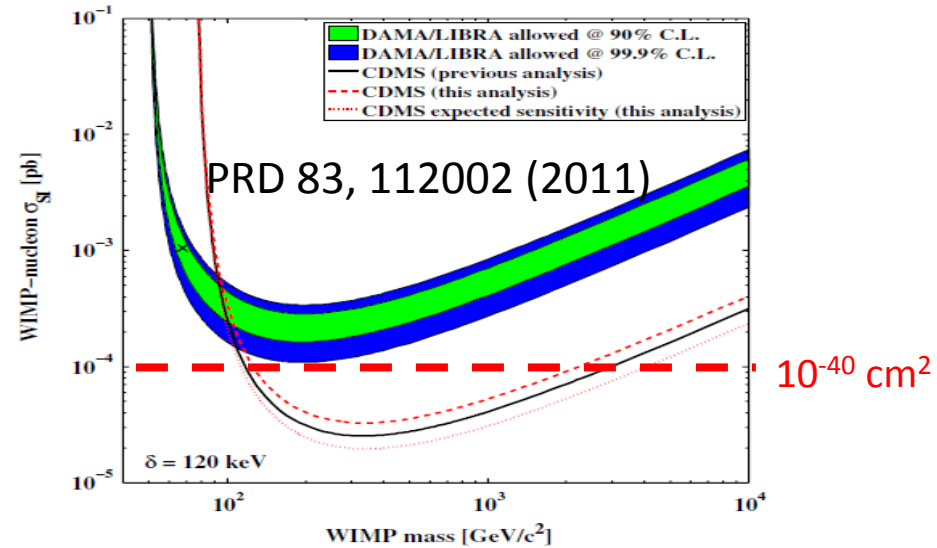
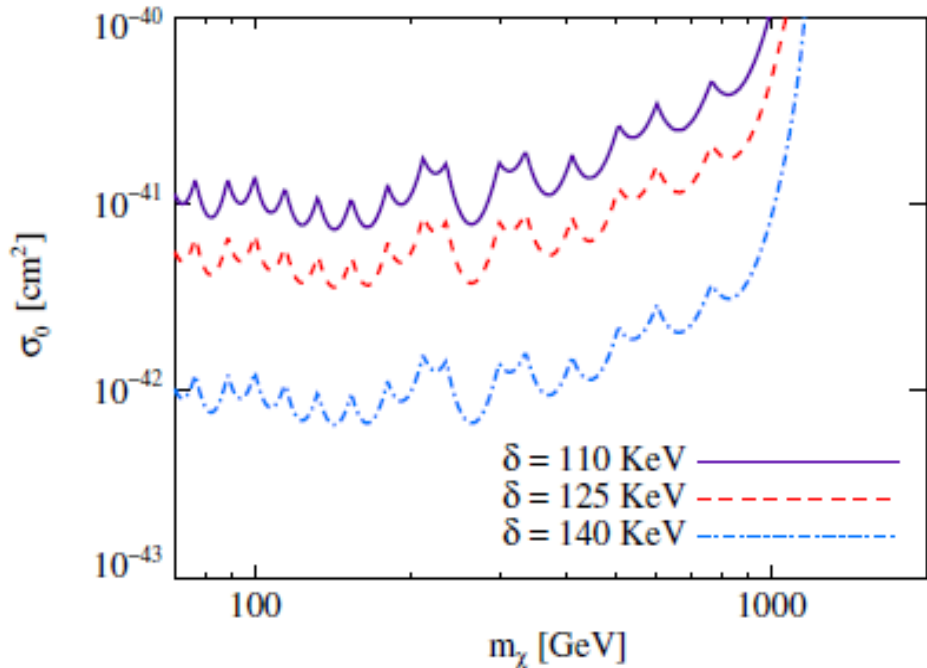
M. Ajello et al., PRD 84, 032007 (2011) arXiv:1107.4272

# Limits on elastic scattering X-section via $\Phi$

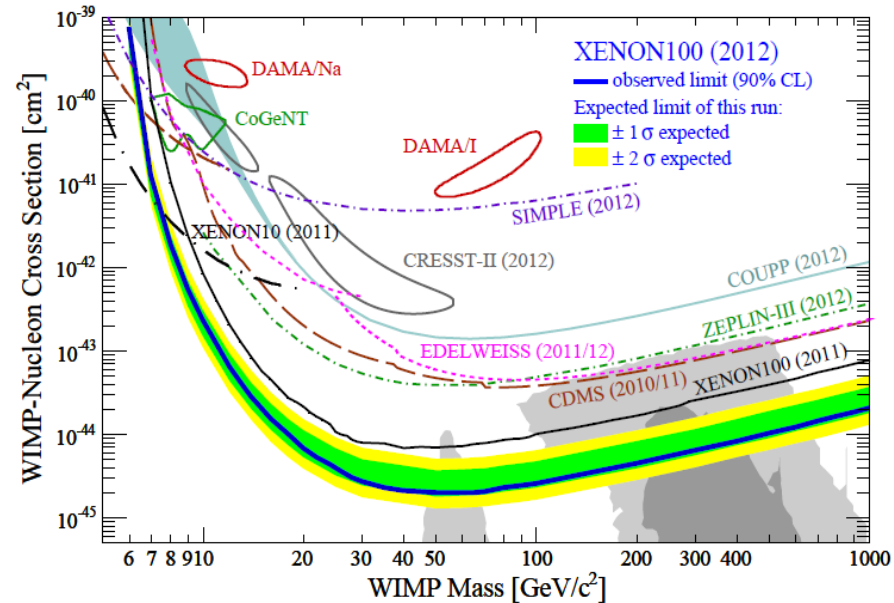


- The limits at 95%CL have been evaluated for three values of the decay length  $L=5 \text{ AU}$ ,  $1 \text{ AU}$ , and  $0.1 \text{ AU}$ 
  - Decreasing  $L$  increases the observed CRE flux by condensing the region within which most decay
  - Even for as large a decay length as  $L = 5 \text{ AU}$ , the signal in the energy range used in this analysis is strongly peaked in the direction of the Sun and extends only a few degrees at most
- “Solar” CRE flux limits correspond to constraints on the rate of decay to CREs outside the Sun that are  $\sim 2\text{-}4$  orders of magnitude stronger than constraints on the associated FSR derived from solar gamma-ray data

# Limits on inelastic scattering X-section

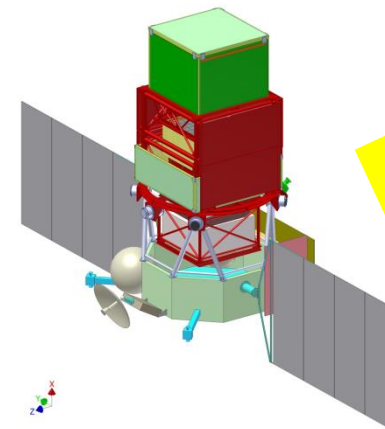
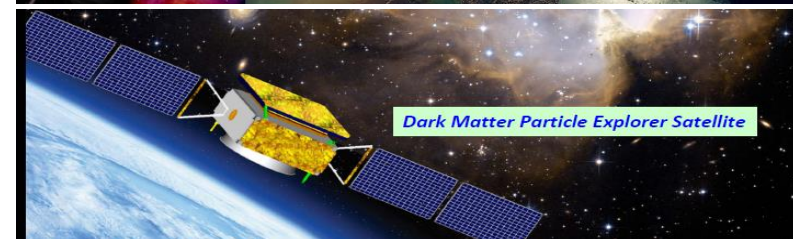
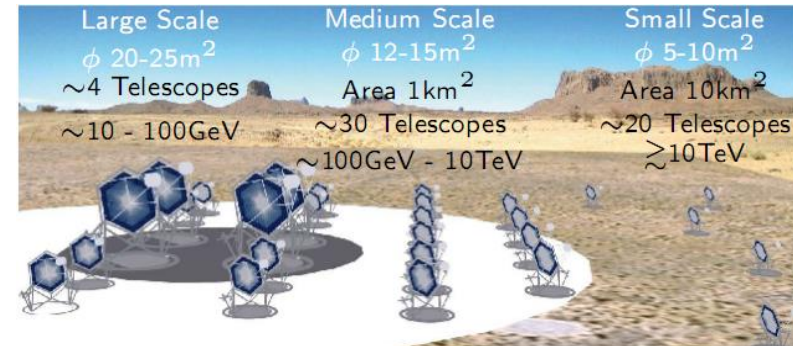


- For a DM particle to scatter inelastically off a nucleon  $N$  via the process  $\chi + N \rightarrow \chi^* + N$ , the DM must have energy  $E \geq \delta (1 + m_\chi/m_N)$ , where  $\delta = m_{\chi^*} - m_\chi$
- The limit at 95%CL have been evaluated with three different  $\delta = 110$  keV, 125 keV and 140 keV



# Next generation gamma ray experiments

- CTA: a km<sup>2</sup> array of Atmospheric Cherenkov telescopes! Sensitivity about a factor 10 better than current ACTs; an energy coverage from a  $\sim 10$  GeV  $\sim 10$  TeV, field of view of up to 10°; angular resolution could be as low as 0.02°
- CALET on ISS : 30 X<sub>0</sub> few % of energy resolution, good angular resolution and high electron/proton separation
  - Launch planned 2014
- DAMPE satellite: 31 X<sub>0</sub> depth calorimeter, few % of energy resolution, good angular resolution and high electron/proton separation
  - Launch planned 2015-2016
- Gamma-400: satellite with better angular and energy resolution in gamma rays + high precision charge particles detector up to several TeV for e- and PeV for protons!
  - launch planned 2018.



See S. Ritz talk

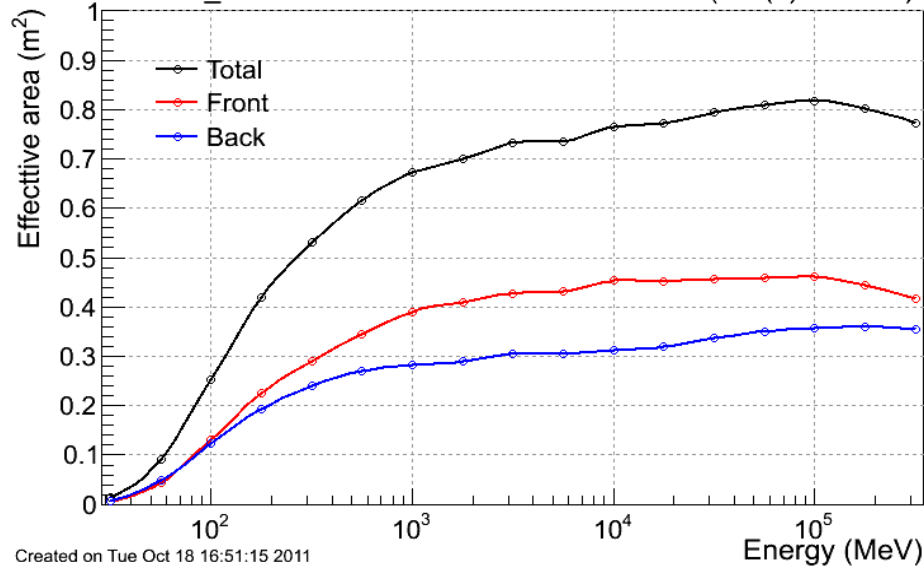
# Summary

- The Fermi LAT team has looked for indirect DM signals using a wide variety of methods
  - So far no signals have been detected and strong constraints have been set
  - No global significant spectral lines from 5–300 GeV in 5 ROIs
    - Uncovered some aspects of the 135 GeV line that require more study
      - Much narrower than expected energy resolution
      - Similar feature seen in Limb
    - Larger than expected systematic uncertainty
    - Does not appear in the inverse ROI
- Other experiments provide DM limits with different methods too
- The next generation of the instruments will provide many other exciting results!
- Many other results are missing in this review (sorry!)
- Thanks to the organizers!

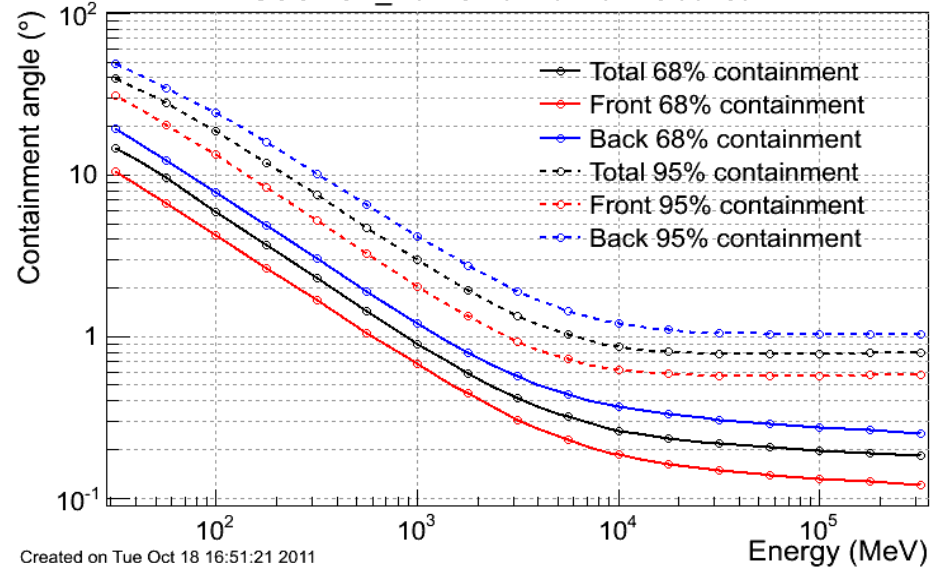
# BACKUP

# Fermi-LAT performance

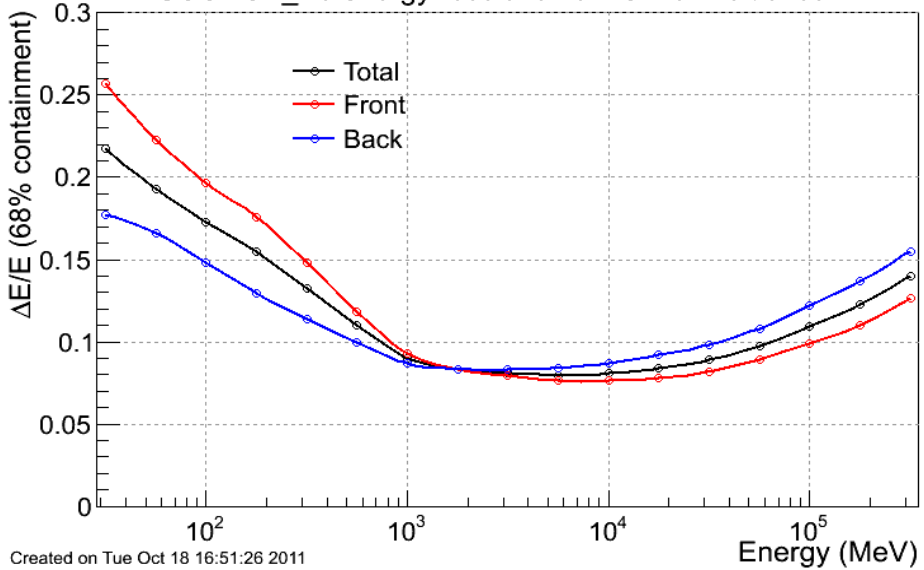
P7SOURCE\_V6 effective area at normal incidence ( $\cos(\theta) > 0.975$ )



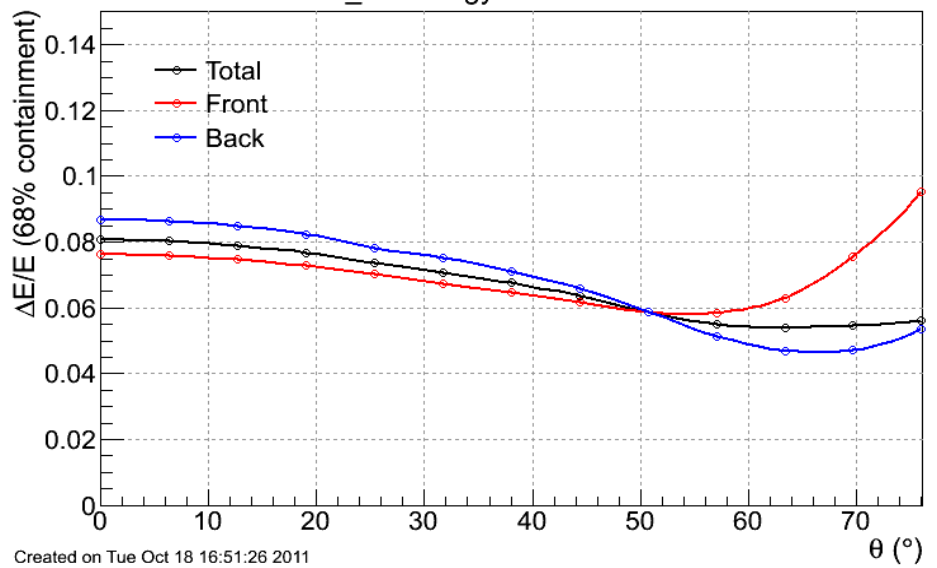
P7SOURCE\_V6 PSF at normal incidence



P7SOURCE\_V6 energy resolution at normal incidence



P7SOURCE\_V6 energy resolution at 10 GeV



# Fermi-LAT Line Search (4 years) systematic

TABLE III. Summary of systematic effects. As stated in the text, we quote either the relative uncertainty of the exposure ( $\delta\mathcal{E}/\mathcal{E}$ ), the relative uncertainty of the number of signal events ( $\delta n_{\text{sig}}/n_{\text{sig}}$ ) or the uncertainty of the induced fractional signal ( $\delta f$ ). We give representative values when the magnitude of the effect depends on energy, or varies between ROIs.

| Systematic                                  |                              | Effect   | Section |
|---|------------------------------|--|---------|
| Effective area scale                        |                              | $\delta\mathcal{E}/\mathcal{E} = \pm 0.1$                | D 1     |
| Averaging exposure over ROI                 | (R3)                         | $ \delta\mathcal{E}/\mathcal{E}  < 0.01$                 | D 1     |
|   | (R180, $E_\gamma = 300$ GeV) | $\delta\mathcal{E}/\mathcal{E} = \pm 0.13$               | D 1     |
| $E_\gamma$ grid spacing                     |                              | $\delta n_{\text{sig}}/n_{\text{sig}} = \pm_{0.1}^{0.0}$ | V A     |
| Energy resolution                           |                              | $\delta n_{\text{sig}}/n_{\text{sig}} = \pm 0.07$        | D 2     |
| Broadening from Z width                     | ( $E_\gamma = 68$ GeV)       | $\delta n_{\text{sig}}/n_{\text{sig}} = -0.07$           | D 3     |
| $P_E$ distribution variation                |                              | $\delta n_{\text{sig}}/n_{\text{sig}} = \pm 0.01$        | D 4     |
| Energy dispersion model $\theta$ -variation |                              | $\delta n_{\text{sig}}/n_{\text{sig}} = \pm 0.02$        | D 4     |
| CR contamination                            | (R3)                         | $ \delta f  < 0.005$                                     | D 5     |
|   | (R180)                       | $\delta f = \pm 0.014$                                   | D 5     |
| Point-source contamination                  |                              | $ \delta f  < 0.005$                                     | D 6     |
| Effective area variations                   | ( $E_\gamma = 5$ GeV)        | $\delta f = \pm 0.005$                                   | D 7 a   |
|   | ( $E_\gamma > 100$ GeV)      | $\delta f = \pm 0.025$                                   | D 7 a   |
| Astrophysical background modeling           | (R180, $E_\gamma = 30$ GeV)  | $\delta f = \pm 0.005$                                   | D 7 b   |
|   | (R180, $E_\gamma > 100$ GeV) | $\delta f = \pm 0.011$                                   | D 7 b   |
|   | (R3)                         | $\delta f = \pm 0.019$                                   | D 7 c   |

TABLE IV. Total magnitude of systematic effects, by ROI and Energy. We obtained these estimates by adding in quadrature the magnitudes of all the potential uncertainties on  $\delta\mathcal{E}/\mathcal{E}$ ,  $\delta n_{\text{sig}}/n_{\text{sig}}$  and  $\delta f$  for each ROI.

| Quantity                               | Energy  | R3                  | R16                 | R41                 | R90                 | R180                |
|--|---------|---------------------|---------------------|---------------------|---------------------|---------------------|
| $\delta\mathcal{E}/\mathcal{E}$        | 5 GeV   | $\pm 0.10$          | $\pm 0.10$          | $\pm 0.11$          | $\pm 0.12$          | $\pm 0.14$          |
| $\delta\mathcal{E}/\mathcal{E}$        | 300 GeV | $\pm 0.10$          | $\pm 0.10$          | $\pm 0.12$          | $\pm 0.13$          | $\pm 0.16$          |
| $\delta n_{\text{sig}}/n_{\text{sig}}$ | All     | $\pm_{0.12}^{0.07}$ | $\pm_{0.12}^{0.07}$ | $\pm_{0.12}^{0.07}$ | $\pm_{0.12}^{0.07}$ | $\pm_{0.12}^{0.07}$ |
| $\delta f$                             | 5 GeV   | $\pm 0.020$         | $\pm 0.020$         | $\pm 0.008$         | $\pm 0.008$         | $\pm 0.008$         |
| $\delta f$                             | 50 GeV  | $\pm 0.024$         | $\pm 0.024$         | $\pm 0.015$         | $\pm 0.015$         | $\pm 0.015$         |
| $\delta f$                             | 300 GeV | $\pm 0.032$         | $\pm 0.032$         | $\pm 0.035$         | $\pm 0.035$         | $\pm 0.035$         |

arXiv:1305.5597



# Fermi-LAT Line Search (4 years) - decay

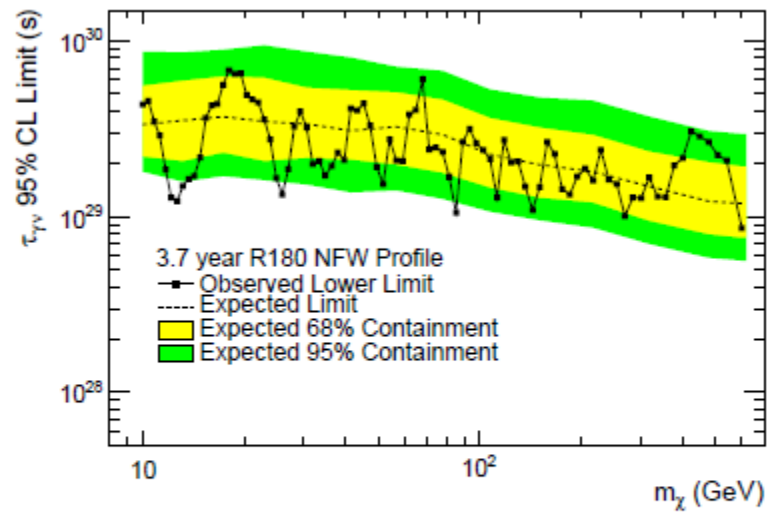
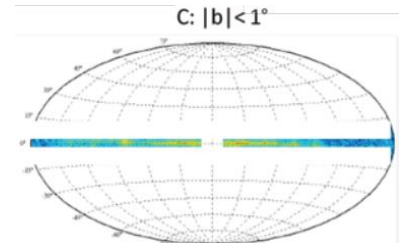
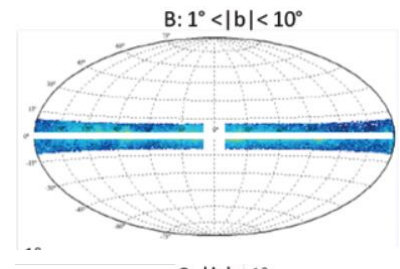
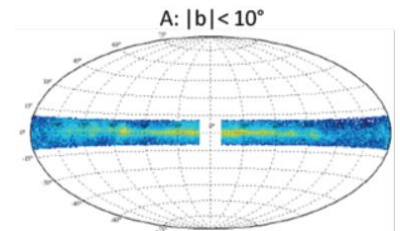
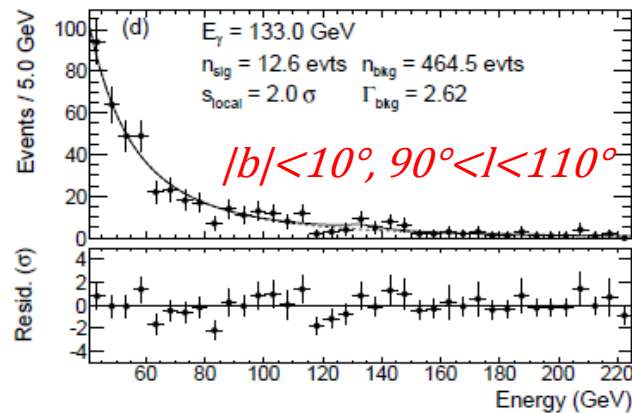
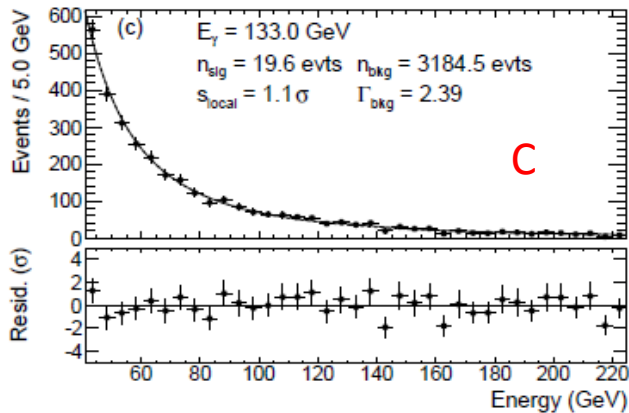
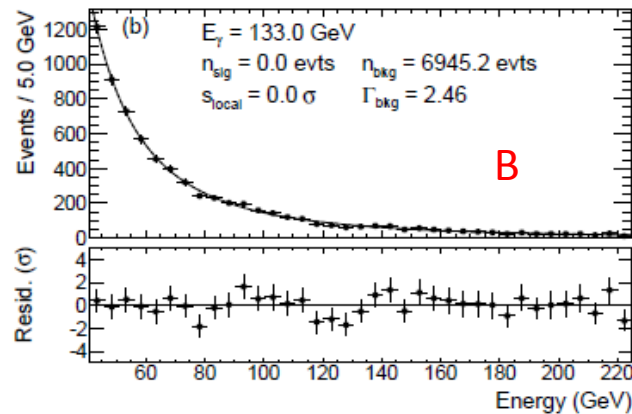
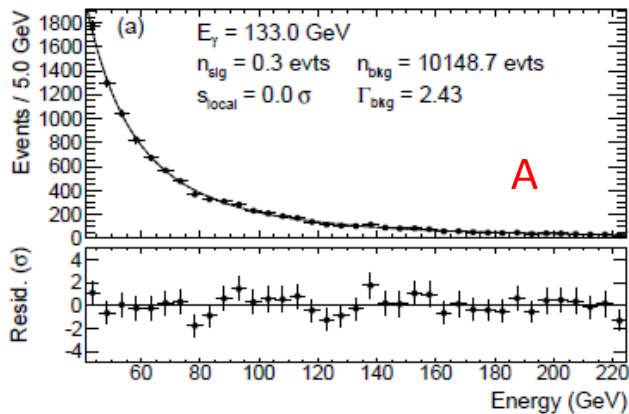


FIG. 10. 95% CL  $\tau_{\gamma\nu}$  lower limits in R180 for an NFW profile. Yellow (green) bands show the 68% (95%) expected containment derived from 1000 single-power-law (no DM) MC simulations. The dashed lines show the median expected limits from those simulations.

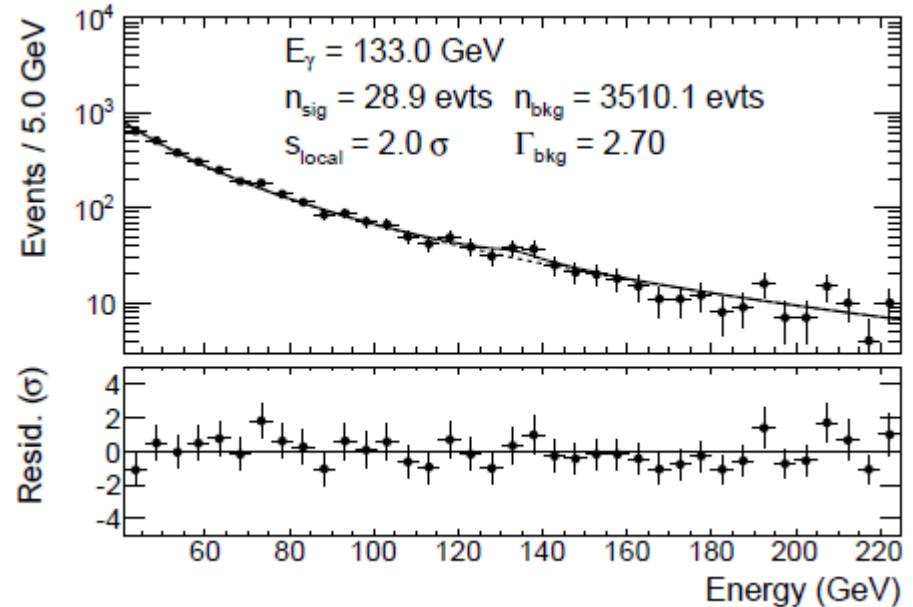
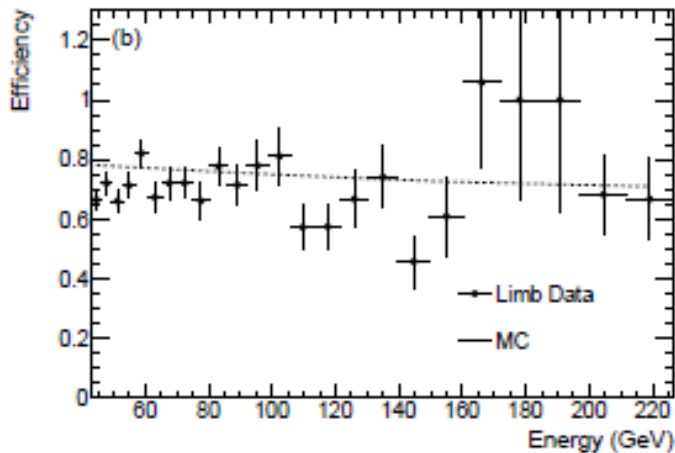
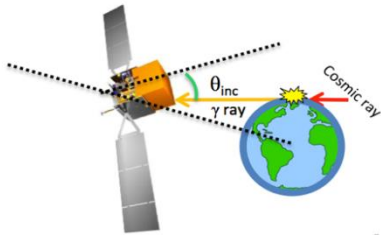
arXiv:1305.5597

# 135 GeV in the inverse ROI spectrum



- No significant feature at 135 GeV seen in inverse ROI searches (2D fits)
- If instrumental cause, then why isn't it in the inverse ROI?
  - Distributions of cut variables in specific ROIs affect cut efficiencies
  - Possible multivariate explanation (might not just be one culprit)
- Investigations still on going

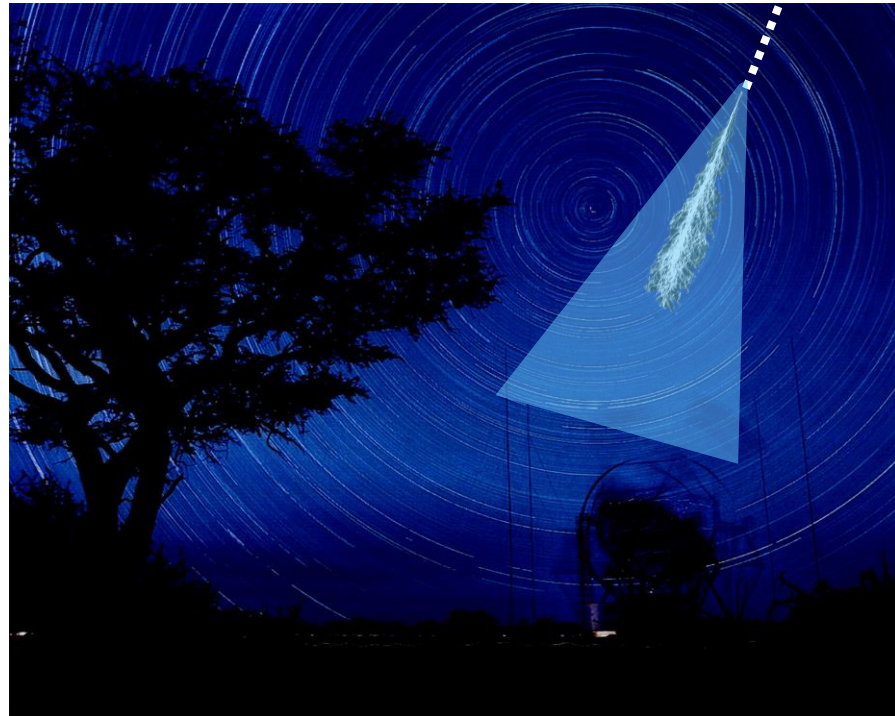
# Earth limb control region



- Study Limb spectrum, which is expected to be a smooth power law
  - No line-like features expected in Limb → from stat. flucs and/or systematics
  - $\delta f_{Aeff}$  ranges from 0.5% to 2.5% (larger at high energies)
- See a slightly larger than average feature at  $\sim 135$  GeV ( $S/N_{limb} \sim 14\%$ )
- Dips in efficiency below and above 135 GeV
  - Could be artificially sculpting the energy spectrum

# Air Cherenkov Telescopes

- Use Cherenkov light from air showers produced from gamma rays interacting with the Earth's atmosphere.
- Use an array of telescopes for improved shower imaging (angular resolution and background rejection)
- Large collecting area ( $\sim 10^5$  m<sup>2</sup> at 100 GeV)
- "Excellent" angular resolution ( $< 0.1$  deg.)
- Threshold at low energy (pushing 100 GeV)
- Limited livetime (moon, zenith angle, etc.)



VERITAS (Arizona)



MAGIC (Canarie)



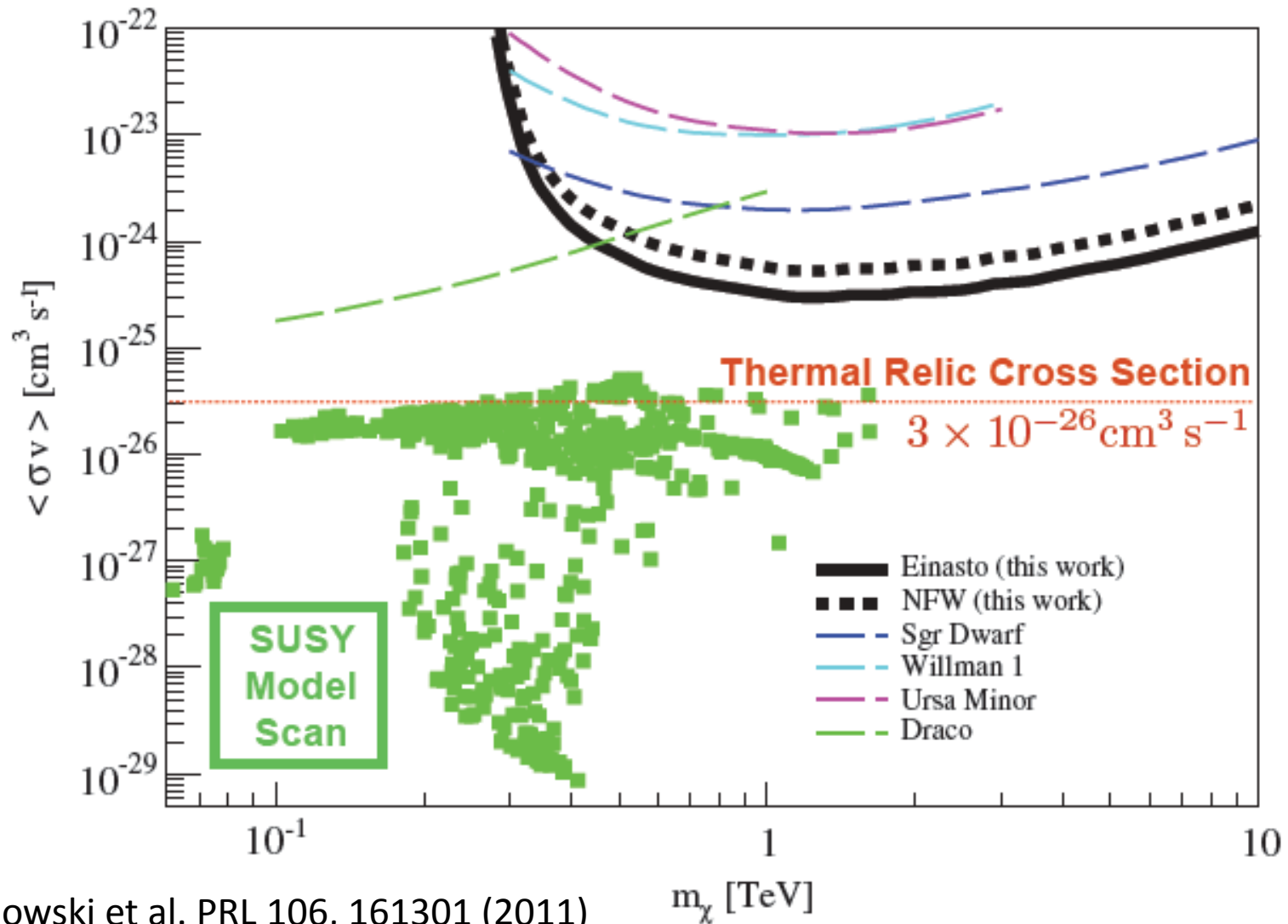
H.E.S.S. (Namibia)



CANGAROO III



# Galactic Center



Abramowski et al. PRL 106, 161301 (2011)

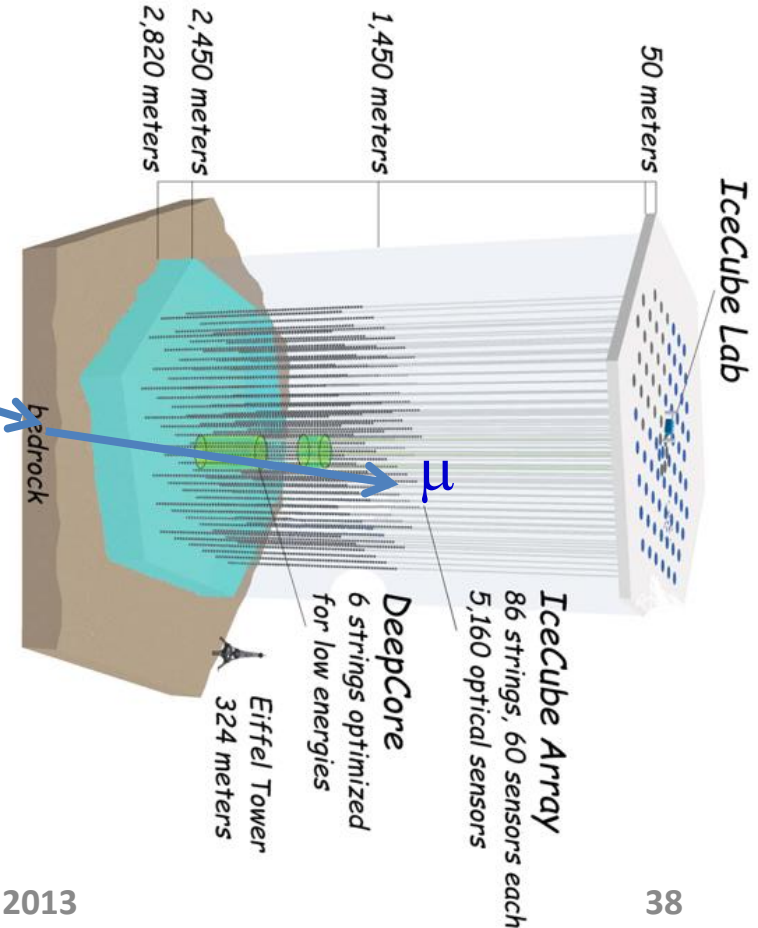
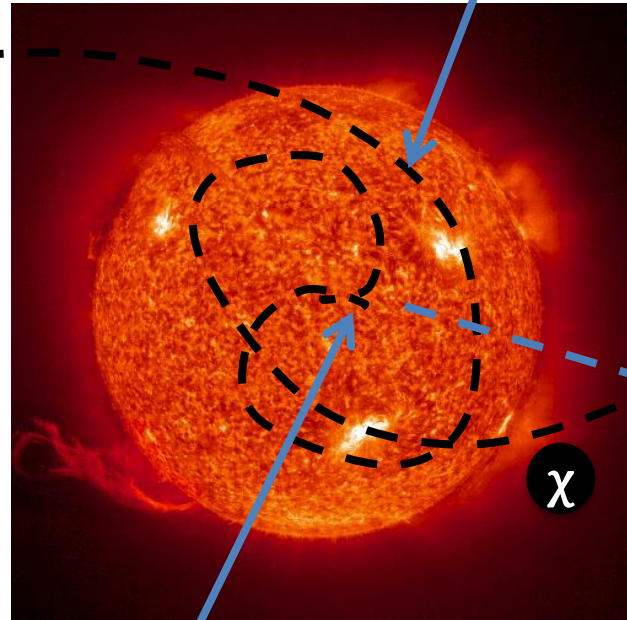
# Neutrinos from the Sun

Combination of direct and indirect detection mechanisms

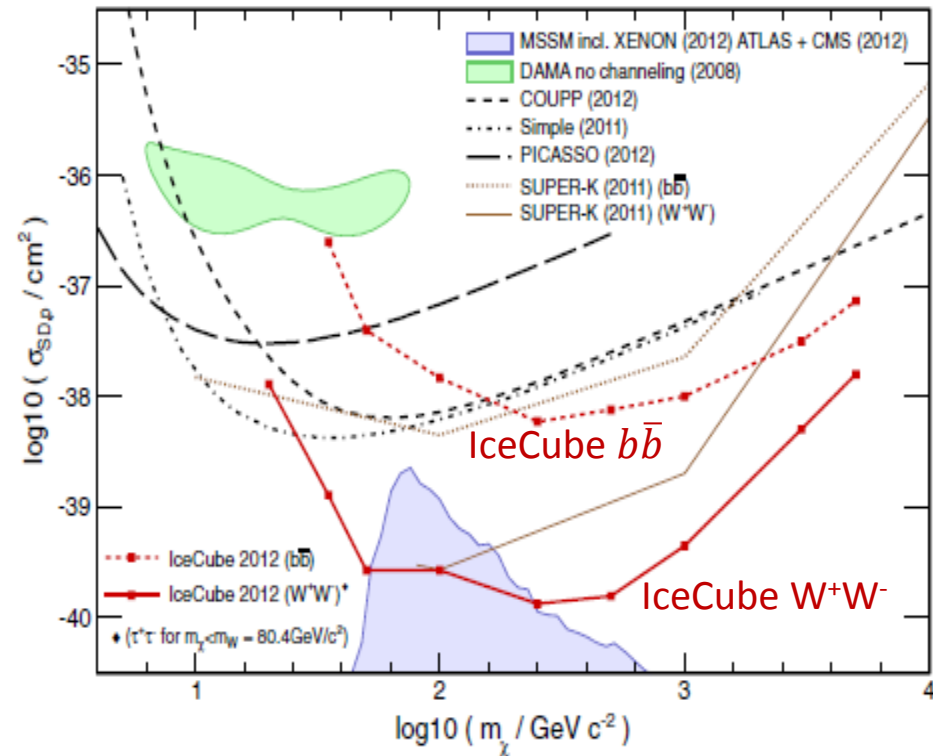
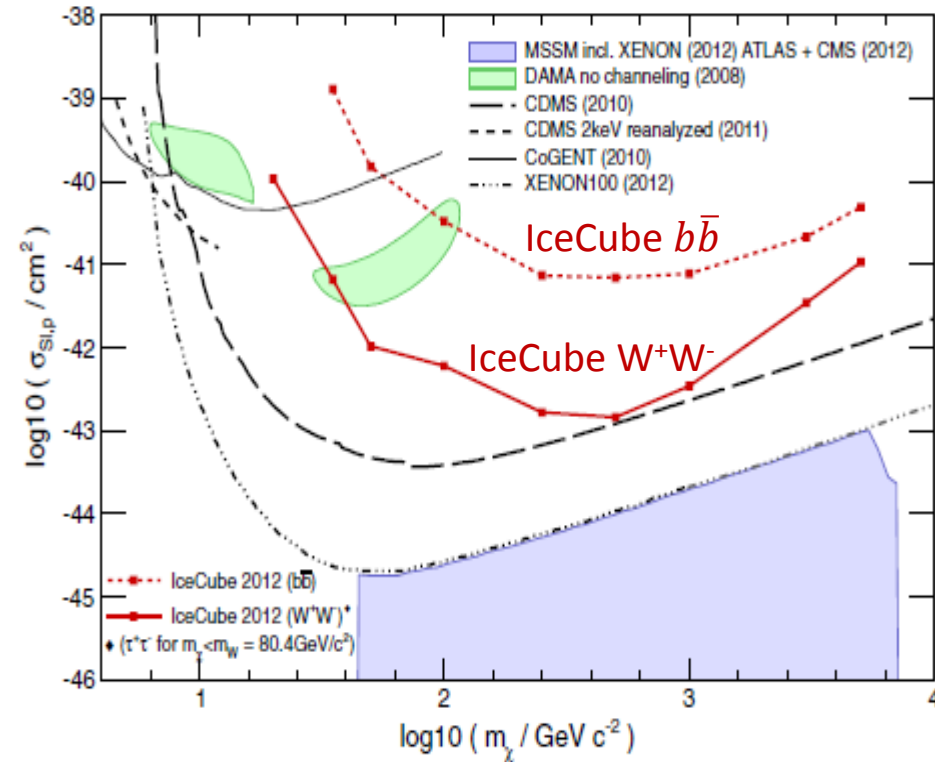
- WIMP-nucleon scattering leads to WIMP capture by the Sun
- WIMP-WIMP annihilation leads to the production of cosmic rays (neutrino)

Nuclear Scattering  
Cross Section  
 $\sigma_{SI}$  or  $\sigma_{SD}$

Self-Annihilation  
Cross Section  $\langle\sigma v\rangle$



# Neutrinos from the Sun

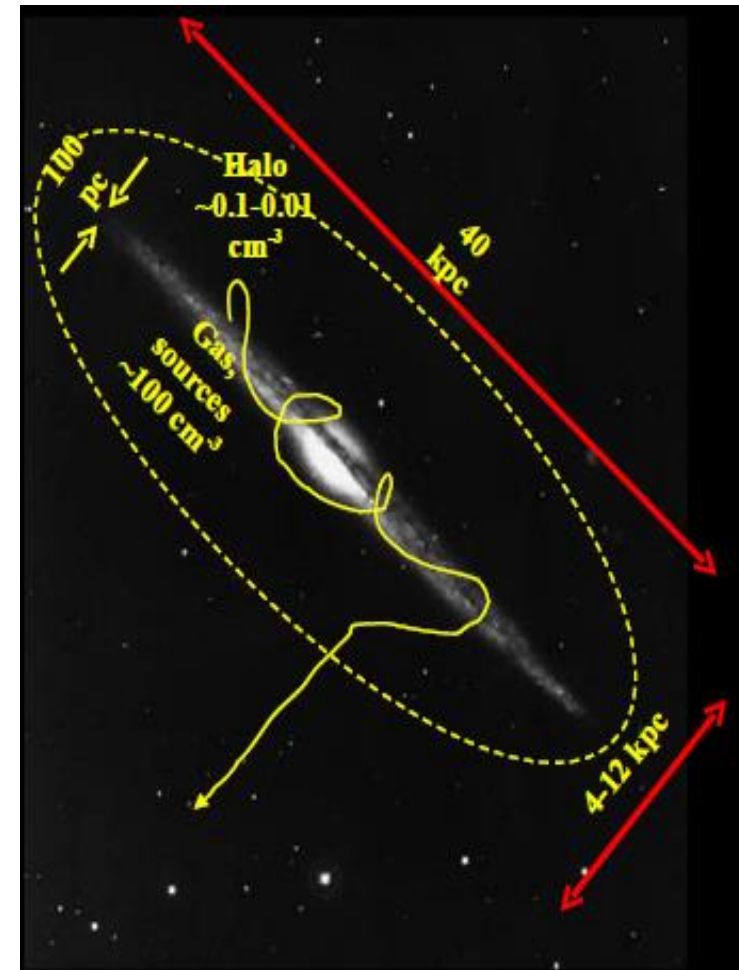


The plots show the 90% C.L. upper limits on Spin Independent (left figure) and Spin Dependent (right figure) for hard and soft annihilation channels over a range of WIMP masses

M. G. Aartsen et al., PRL 110, 131302 (2013)

# Galactic cosmic rays

- High-energy (GeV–TeV) charged primary Cosmic Rays (CRs) are believed to be produced in our galaxy, most likely in Supernova Remnants (SNRs)
- CRs injected into ISM propagate for millions of years before escaping to intergalactic space
- Particle interactions with interstellar gas, radiation and magnetic fields produce EM radiation from radio to gamma rays, and other secondaries ( $e^\pm$ , nuclei, etc.)
- During the transport from their source of origin to our solar system, CRs scatter on random and irregular components of the  $\mu\text{G}$  Galactic Magnetic Field (GMF), which almost isotropize their directions.
- Contrary to hadronic CRs, high-energy ( $>\text{GeV}$ ) Cosmic Ray Electrons and Positrons (CREs) propagating in the GMF lose their energy rapidly through synchrotron radiation and by inverse Compton collisions with low-energy photons of the interstellar radiation field.





# CRE propagation equation

- For CREs the convection and reacceleration could be neglected above few GeV, so that the propagation of CREs can be expressed in terms of usual conservation equation:

$$\frac{\partial N}{\partial t} - \vec{\nabla} \cdot \left( D \vec{\nabla} N \right) - \frac{\partial}{\partial E} (bN) = q$$

- $b$  is the continuous energy loss rate,  $b \approx 1.4 \times 10^{-16} \text{ GeV}^{-1} \text{ s}^{-1}$
- $D$  is the diffusion coefficient,  $D = D_0 (E/E_0)^\delta$ 
  - $D_0 \approx 5.8 \times 10^{28} \text{ cm}^2 \text{ s}^{-1}$ ,  $\delta = 1/3$  and  $E_0 \approx 4 \text{ GeV}$
- CREs lose almost all of their energy  $E$  after a time  $T$ :
  - $T = 1/bE \approx 2 \times 10^5 \text{ yr}/E(\text{TeV})$
- CREs can diffuse over a distance  $R = (2DT)^{1/2}$  during the lifetime  $T$ 
  - $R \approx 1.6 (0.75) \text{ kpc}$  for  $E = 100 \text{ GeV}$  ( $1 \text{ TeV}$ )
- Such high-energy CREs might originate from a highly anisotropic collection of a few nearby sources

# Anisotropy

- Degree of anisotropy: 
$$\delta = \frac{I_{\max} - I_{\min}}{I_{\max} + I_{\min}}$$

where  $I_{\max(\min)}$  is the maximum (minimum) intensity

- In case of the dipole anisotropy:  $I(\theta) = I_0 + I_1 \cos(\theta) \Rightarrow \delta = I_1/I_0$

- The anisotropy due to the pure diffusion term is given by: 
$$\delta = \frac{3D}{c} \frac{|\vec{\nabla} N|}{N}$$

- In case of a single source of age  $t_i$  at the position  $r_i$  (burst-like injection) the spectrum of CREs at the solar system is 
$$\propto \exp\left(-\frac{r_i^2}{r_{diff}^2}\right)$$
 (Green's function)

- So that, its contribution to the anisotropy is given by:

$$\delta_i = \frac{3D}{c} \frac{2|\vec{r}_i|}{r_{diff}^2} \Rightarrow \delta_i = \frac{3|\vec{r}_i|}{2ct_i}$$

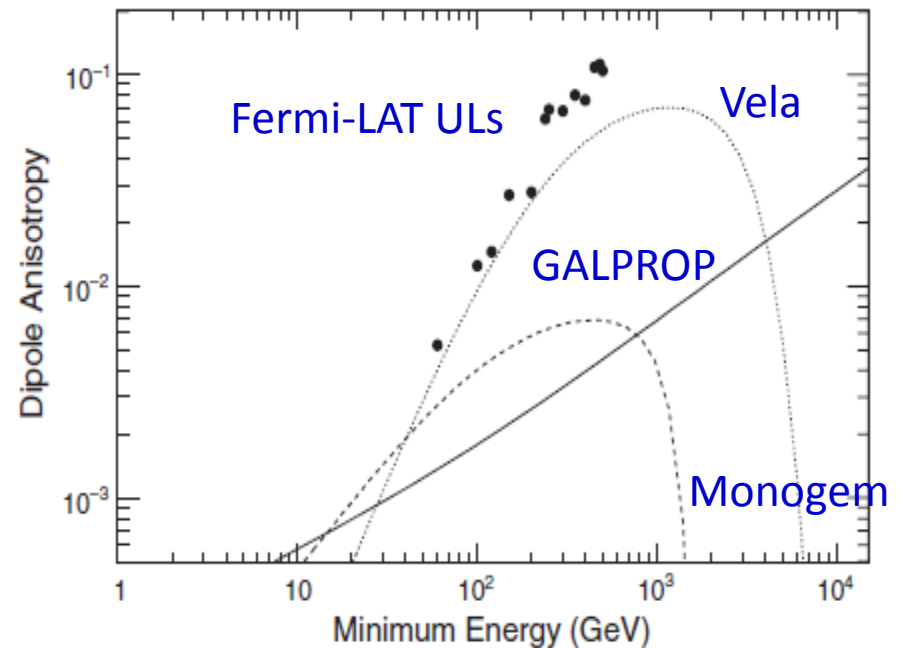
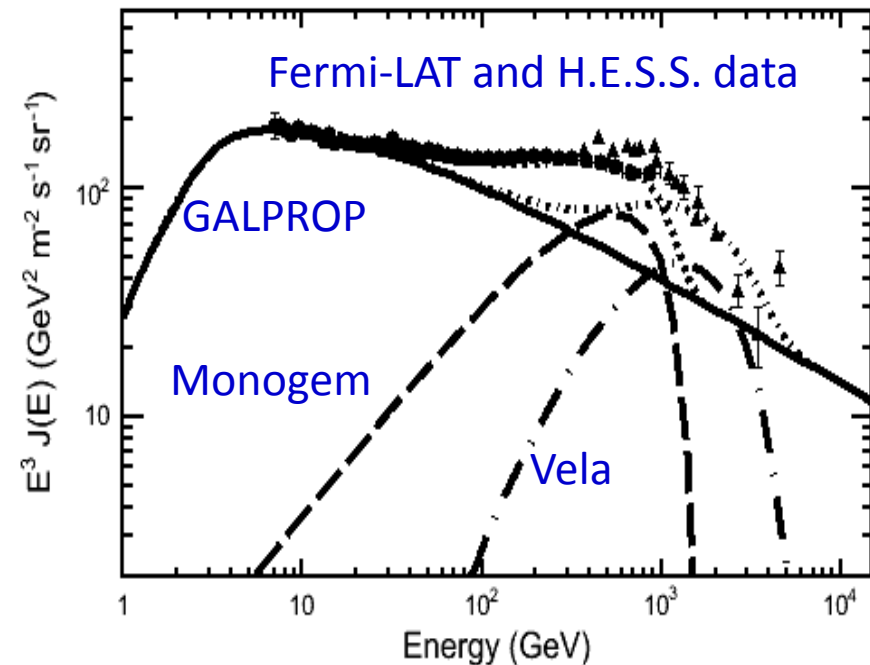
- The total anisotropy due to a distribution of point-like sources in the sky is then given by:

$$\delta = \frac{\sum_i N_i \delta_i \hat{r}_i \cdot \hat{n}_{max}}{\sum_i N_i}$$

where  $n_{max}$  is the direction of maximum intensity

# CRE Fermi-LAT spectrum

- Hard to fit the CRE spectrum with a single-component diffusive model
- Good fit possible with an additional high-energy component
  - If it's an  $e^+/e^-$  source (e. g. nearby pulsars or dark matter), the Fermi spectrum and Pamela positron fraction can be simultaneously fitted
- For single sources (e.g. Vela-like and Monogem-like) the value of the injected luminosity is such that the total flux is not higher than the one measured by the Fermi-LAT and H.E.S.S.
- For each source, the anisotropy has been evaluated assuming that the contributions to the anisotropy from all remaining sources are negligible



# ... and DM scenario

The positron excess detected by PAMELA can be ascribed not only to astrophysical sources such as pulsars, but also to the annihilation or decay of Galactic dark matter

